藥學博士 學位論文

간세포 생존의 PKA 연계 조절 경로와 약물학적 응용

Novel PKA-associated pathways for the regulation of hepatocyte survival and pharmacological applications

2017년 8월

서울대학교 대학원

약학과 약물학전공

吳 宏 敏

Abstract

간세포 생존의 PKA 연계 조절 경로와 약물학적 응용

Novel PKA-associated pathways for the regulation of hepatocyte survival and pharmacological applications

Hong Min Wu

Advisor: Prof. Sang Geon Kim

Hepatocytes are primary targets for toxic insults such as drugs, alcohol and viruses. Hepatocyte death is evident and a common feature in a variety of liver disease ranging from drug induced liver injury, viral/alcoholic/autoimmune hepatitis to metabolic disorders. Therefore, preserving functional hepatocytes is important for intervention and amelioration of liver injury. Currently, therapeutic approaches targeting hepatocyte death are challenging from the lower clinical outcomes. Thus, molecular targets and pathways related to hepatocyte survival need to be discovered. Protein kinase A (PKA) mediates the molecular signaling transduction between receptors/therapeutic drugs and cellular targets. The numerous targets associated with PKA determine its nature as an important regulator for energy metabolism. The aims of this study are to explore novel molecules associated with PKA pathway targeting hepatocyte survival and specify the

molecules and underlying mechanisms.

As an aim to find a pharmacological approach aiming at PKA-associated pathway, this study investigated the possibilities of methylene blue (MB), a mitochondria-targeting drug in hepatocyte protection. MB treatment resulted in a PKA-dependent activation of liver kinase B 1 (LKB1). LKB1 then induced activation of AMP-activated protein kinase (AMPK) that caused inhibitory phosphorylation of glycogen synthase kinase 3 β (GSK3β). MB treatment also induced an AMPK-independent early inhibition of GSK3β. siRNA knockdown of PKA eliminated the inhibitory phosphorylation of GSK3β by MB, suggesting the early inhibition of GSK3β by MB is dependent on PKA. Together, the ability of MB in protecting hepatocytes and liver against toxicant induced injury was confirmed by both *in vitro* and *in vivo* experiments. These results support the notion that MB facilitates dual inhibition of GSK3β downstream of PKA, and protects hepatocyte.

Liver X receptor α (LXRα) is a nuclear receptor and oppositely regulates lipid metabolism and inflammation. In the analysis of public gene expression omnibus (GEO) database, LXRα level significantly decreased in different injury conditions in hepatocytes, mice and human liver. LXRα agonist treatment attenuated CCl_4 induced hepatocyte injury, whereas LXR$\alpha^{-/-}$ mice had more hepatocyte death and liver injury in response to CCl_4, indicating LXRα's protective effects on hepatocytes. In an additional bioinformatics study, LXRα protection of hepatocytes may result from antagonizing transforming growth factor β (TGFβ) signaling, which was confirmed by subsequent

experiments using AML12 cell and mouse primary hepatocytes. Immunoblotting, quantitative real-time polymerase chain reaction (qRT-PCR), reporter gene assay and chromatin immunoprecipitation (ChIP) analysis were used to study molecular mechanism downstream of LXRα. Cannabinoid receptor 2 (CB2) was identified as a transcriptional target of LXRα. CB2 contributed to LXRα's protective effects on hepatocytes via upregulation of microRNA-27b (miR-27b). MiR-27b was demonstrated here as a novel upstream inhibitory regulator of ubiquitin specific peptidase 4 (USP4), a deubiquitylating enzyme for TGFβ receptor 1 (TβRI). In addition, the changes on USP4 and TβRI by CB2 agonist were attenuated by PKA inhibition. Finally, albumin promoter-driven lentiviral delivery of LXRα protected hepatocytes from injury. Together, LXRα transcriptionally upregulates CB2, leading to miR-27b upregulation and contributes to protecting hepatocytes via repression of USP4 and TβRI.

Taken together, the outcomes of this study demonstrate not only PKA-dependent GSK3β inhibition for hepatocyte survival activated by pharmacological agent, but also CB2-mediated PKA pathway associated with LXRα for hepatocyte protection, providing novel exogenous and endogenous pathways and pharmacological insights for hepatocyte survival, and potentially for the cure of liver diseases.

Keywords: Hepatocyte injury, PKA, LXRα, CB2, methylene blue, AMPK

Student Number: 2009-24034

Table of contents

List of table and figures

List of abbreviations

ACC: Acetyl-CoA carboxylase

ALT: Alanine aminotransferase

AMPK: AMP-activated protein kinase

AST: Aspartate aminotransferase

CB2: Cannabinoid receptor 2

ChIP: Chromatin immunoprecipitation

ChREBP: Carbohydrate-responsive element-binding protein

CHX: Cycloheximide

COX2: Cyclooxygenase 2

DEGs: Differentially expressed genes

DMEM: Dulbecco's modified eagle's medium

FBS: Fetal bovine serum

GEO: Gene expression omnibus

GR: Glucocorticoid receptor

GSK3β: Glycogen synthase kinase 3 β

H&E: Hematoxylin & Eosin

IL1β: Interleukin 1 β

iNOS: Inducible nitric oxide synthase

LKB1: Liver kinase B1

LXR: Liver X receptor

LXRE: LXR response element

MB: Methylene blue

MiR-27b: MicroRNA-27b

PKA: Protein kinase A

PI: Propidium iodide

qRT-PCR: quantitative real-time polymerase chain reaction

ROS: Reactive oxygen species

SREBP-1c: Sterol regulatory element-binding protein 1c

TβRI: TGFβ receptor 1

TGFβ: Transforming growth factor β

TNFα: Tumor necrosis factor α

USP4: Ubiquitin specific peptidase 4

I. Introduction

Everyday billions of cells undergo programmed death, and meanwhile new cells are proliferated to keep the functionality of whole organism. The balance between cell death and proliferation is essential for organ development and tissue homeostasis. When the balance is broken, many unwanted results will happen. Too much cell death can lead to acute pathologies such as liver failure and heart attack, whereas too much cell proliferation will cause cancer development (Fischer and Schulze-Osthoff, 2005). In fact, the imbalance between cell death and replacement contributes to almost half of the medical diseases, and many of them are lack of proper therapy (Fischer and Schulze-Osthoff, 2005).

The primary liver cells, hepatocytes, are the first target for various injury stimuli, and repetitive hepatocyte injuries facilitate liver disease development (Inokuchi et al., 2010; Takehara et al., 2004). Insults on hepatocytes trigger hepatocyte death signaling pathways, which can cause the activation of neighboring macrophage and hepatic stellates cells for the progression of inflammation, fibrosis, and cirrhosis (Martin-Murphy et al., 2010; Watanabe et al., 2007). Hepatocyte death is a common phenomenon in many liver diseases (Feldstein et al., 2003; Natori et al., 2001), therefore, methods to preserve functional hepatocytes may provide therapeutic strategies for liver protection.

During the past few decades, many apoptosis-based therapies have been developed for liver disease treatment. The therapies mainly target to the key players in cellular apoptosis regulation. These key players include death receptors (e.g., tumor necrosis factor (TNF) receptor), mitochondrial pathway gatekeepers (e.g., Bcl-2 family proteins) and the apoptosis executioner enzymes (e.g., caspases). The anti-TNF therapy has been suggested effective in alcohol mediated liver injury (Iimuro et al., 1997). However, whether anti-TNF therapies is beneficial for liver disease remains to be determined because long duration of blocking TNF activity is related to impaired liver regeneration (Tilg et al., 2003). Genasense (an antisense oligonucleotide for Bcl-2) is under preclinical trials for the treatment of different cancer (Hall et al., 2013; Bedikian et al., 2014), and its application on liver cancer remain to be explored. Caspase inhibitor has been reported with potential effects in the treatment of hepatitis and liver fibrosis (Pockros et al., 2007). However, it fails to prevent apoptosis in some specific experimental settings such as caspase-independent apoptosis (Hirsch et al., 1997). Collectively, these therapeutic approaches targeting hepatocyte death/survival are challenging, and new molecular targets for hepatocyte survival and the detail of regulatory mechanisms remain to be explored.

Protein kinase A (PKA) is an intracellular second messenger cAMP-dependent kinase and cAMP/PKA pathway represents one primary pathway in transmitting the cell external signaling into internal environment. The cAMP/PKA signalling system is

important for energy homeostasis by regulating a wide range of intracellular processes. (Francis and Corbin, 1994). In liver, PKA regulates lipid metabolism by inhibitory phosphorylating sterol regulatory element-binding protein 1c (SREBP-1c) and carbohydrate-responsive element-binding protein (ChREBP), key enzymes regulating lipogenesis (Lu and Shyy, 2006; Kawaguchi et al., 2001), and inhibits Toll-like receptor 4 response by suppressing Tumor necrosis factor α (TNFα) *in vitro* (Wall et al., 2009). In addition, activation of cAMP-PKA signaling prevents hepatocyte death in mice from ischemia/reperfusion injury (Ji et al., 2012), as well as hepatocyte apoptosis induced by death receptor agonist *in vitro* (Wang et al., 2006). However, the molecular signaling associated with PKA in hepatocytes is still not fully understood.

Methylene blue (MB) was first synthesized in 1876 and had a long history with many applications both as staining reagent and medications (Schirmer et al., 2011). The first medical use of MB is treatment of malaria during the world wars, and was later disliked by the soldiers because of the blue color (Parascandola, 1981). From the 1890s to 1930s, MB's various effects have been discovered, including its antidepressant, antifungal activities, and treatment for methemoglobinemia and cyanide toxicity (Ohlow and Moosmann, 2011; Alston, 2014). Around 1970s, MB was found can speed up cytochrome c reduction (Weinstein et al., 1964). Later, MB was found has the unique auto-redux property of spontaneous cycling between the oxidized blue color form (MB) and reduced colorless form (LeucoMB) (Weinstein et al., 1964; Schirmer et al., 2011).

MB accepts electrons from NAD(P)H and $FADH_2$ and is reduced into LeucoMB. At the same time LeucoMB can be reoxidized into MB by O_2 (Atamna et al., 2008). The special auto-redox feature of MB enabled people to investigate its therapeutic effect on mitochondrial dysfunction related diseases. Nowadays, MB has been considered as a mitochondria-targeting compound that integrates the electron leaked from mitochondrial electron transport (Gabrielli et al., 2004; Atamna et al., 2008). Consequently, MB can help avoiding excess reactive oxygen species (ROS) production, enhancing the mitochondrial β oxidation and improving total mitochondrial function (Atamna et al., 2008; Visarius et al., 1999). Currently, MB has been widely investigated for clinical therapy of mitochondrial dysfunction related diseases such as Alzheimer's diseases (Oz et al., 2009). Nevertheless, whether MB can prevent toxicant induced hepatocyte and liver injury has not been examined yet.

Mitochondrial dysfunction can lead to hepatocyte death through accelerating ROS accumulation and oxidative stress. Oxidative stress induces loss of mitochondrial membrane potential, dysregulated redox homeostasis, disruption of ATP synthesis and ultimately triggers hepatocyte death (Li et al., 2016). Thus, excessive oxidative damage is related to many liver diseases from fatty liver, hepatitis to liver fibrosis/cirrhosis and hepatocellular carcinoma (Li et al., 2016). AMP-activated protein kinase (AMPK) is an intracellular energy that can regulate mitochondrial function. AMPK is activated through phosphorylating at Thr-172 residue in response to high AMT/ATP ratio. Liver

kinase B 1 (LKB1) and calcium/calmodulin-dependent protein kinase kinase (CaMKK) are two identified upstream kinases for AMPK phosphorylation (Hawley et al., 2003; Hurley et al., 2005). Activated AMPK affects intracellular redox state. AMPK can increase mitochondrial biogenesis through activating peroxisome proliferator-activated receptor γ coactivator-1 α (Chaube et al., 2015). AMPK can also enhance β-oxidation of fatty acid and participate in mitochondrial ATP generation (Hardie et al., 2012). In addition, AMPK directly regulates cellular redox state through induction of mitochondrial antioxidant enzymes (Xie et al., 2008). Many antioxidants such as metformin, polyphenols and flavonoids have been shown to protect mitochondria and hepatocytes through AMPK activation (Shaw et al., 2005; Kim et al., 2012; Choi et al., 2010). Since MB is a mitochondria-targeting drug, its possibility to activating AMPK may provide research value for targeting hepatocyte survival and preserving functional hepatocytes.

Liver X receptors (LXRs) belong to the nuclear receptor family and are members of transcription factors. Identified endogenous ligands for LXRs are 24S, 25, and 27 hydroxycholesterol (Apfel et al., 1994; Venkateswaran et al., 2000). LXRs act as cholesterol sensor and are activated by increased intracellular cholesterol concentration. Activated LXRs promote cholesterol efflux and decrease intracellular cholesterol synthesis, as a result, increase the net elimination of cholesterol in the liver (Repa et al., 2000b). As a transcription factor, LXRs bind to the LXR response element (LXRE) to

regulate downstream genes expression (Apfel et al., 1994). Many LXRs target genes have been identified. *Cyp7a1*, the first identified LXRs target gene in mouse, promotes bile acid synthesis (Peet et al., 1998). Subsequent studies demonstrated LXRs' ability in promoting reverse cholesterol transport by transcriptionally regulate *ABCA1* and *ABCG* family genes (Repa et al., 2000b; Kennedy et al., 2005). Besides cholesterol metabolism regulation, LXRs are also found have important roles on lipogenesis via transcriptional regulation of lipogenesis related genes (e.g., *SREBP-1c*, *Fas* and *Scd1*) (Repa et al., 2000a; Joseph et al., 2002; Chu et al., 2006). LXRs also have effects on glucose metabolism. For example, LXRs promote glucose uptake via induction of *GLUT4* (Dalen et al., 2003), and inhibit hepatic gluconeogenesis via downregulating *PEPCK* (Cao et al., 2003). Consequently, LXRs activation improves glucose tolerance and insulin sensitivity (Laffitte et al., 2003). Thus, LXRs are critical metabolism regulator and charge whole-body energy homeostasis via regulating cholesterol, lipid and glucose metabolism at many levels.

There are two identified isoforms of LXRs, LXRα and LXRβ. Comparing to the ubiquitously expressed LXRβ, LXRα is found mainly in liver, adipose tissue, macrophages and intestine (Kohro et al., 2000). In this study, we focused on the study of LXRα since it is the major form in hepatocytes (Kohro et al., 2000). LXRα is the master regulator of *de novo* lipogenesis and activation of LXRα leads to triglyceride accumulation (Schultz et al., 2000). However, there are also increasing evidence

showing LXRα's beneficial effects on anti-atherogenesis, cholesterol removal and anti-inflammation (Tangirala et al., 2002; Uppal et al., 2007). In several animal or cell models, the lack of LXRα aggravates liver inflammation and fibrosis (Joseph et al., 2003; Beaven et al., 2011), but the role of LXRα for the protection against hepatocyte injury and whether PKA is involved in the process have not yet been elucidated.

In the present work, the research aims are 1) to find a pharmacological approach aiming at PKA-associated pathway, and 2) to address the impact of LXRα on hepatocyte survival and investigate whether PKA is involved. First, studies were done on investigating MB's ability in maintaining hepatocyte viability and preventing toxicant induced hepatitis, as well as the unexplored molecular basis. MB activated liver kinase B 1 (LKB1)-AMP-activated protein kinase (AMPK) pathway downstream of PKA. Activation of AMPK by MB caused inhibitory phosphorylation of glycogen synthase kinase 3 β (GSK3β) at later stage. Moreover, MB mediated GSK3β inhibition at earlier stage is directly dependent on PKA. Thus, it was shown here that MB could lead a dual inhibition of GSK3β downstream of PKA. Secondly, LXRα's impact on hepatocyte protection and the role of PKA in LXRα-related molecular signaling transduction were determined. LXRα agonist attenuated toxicant induced hepatocyte and liver injury, whereas absence of LXRα exacerbated that. Bioinformatics study and *in vitro* experiments demonstrated that LXRα protected hepatocyte via inhibiting transforming growth factor β (TGFβ) signaling. In liver injury conditions, cannabinoid

receptor 2 (CB2) positively correlated with LXRα, and subsequent experiments proved that *Cb2* was a target gene of LXRα. Further molecular studies uncovered that LXRα-CB2 inhibited TGFβ signaling via ubiquitin specific peptidase 4 (USP4) repression, an event mediated by microRNA-27b (miR-27b) upregulation. In addition, USP4 repression by CB2 agonist was PKA-dependent. These results provide a novel LXRα-associated pathway in modulating the fate of hepatocytes, via regulating CB2 and suppressing USP4 mediated TGFβ signaling. Finally, to connect the molecular pathways demonstrated here with pharmacological applications, the effects of MB and LXRα in protecting against hepatocyte and liver injury were tested. As a result, MB can prevent toxicant-induced hepatocyte apoptosis and hepatitis; hepatocyte-specific delivery of LXRα ameliorated hepatocyte apoptosis. These results may provide attractive therapeutic targets and strategy for the prevention and cure of liver diseases.

II. Materials and methods

1. Materials

GW3965 (for cell-based assay), PI, MG132, MTT, DCFH-DA, anti-actin antibody and anti-ubiquitin antibody were supplied from Sigma (St. Louis, MO). TGFβ1 was purchased from Humanzyme (Chicago, IL). FITC-Annexin V, anti-phospho-Tyr216-GSK3β and anti-iNOS antibodies were from BD Bioscience (San Jose, CA). Anti-caspase 3, anti-Myc, anti-LXRα (for ChIP assay), anti-TβRI, anti-USP4, anti-COX2 and anti-PKA antibodies were supplied from Santa Cruz Biotechnology (Santa Cruz, CA). Antibodies directed against cleaved-caspase 3, cleaved-PARP, phospho-AKT, AKT, phospho-Smad2, Smad2, phospho-Smad3, Smad3, Flag-tag, phospho-LKB1, LKB1, phospho-AMPK, AMPK, phospho-ACC, ACC, phospho-Ser9-GSK3β and GSK3β were obtained from Cell Signaling (Beverly, MA). Anti-LXRα (for immunoblotting) was provided from Thermo Scientific (Waltham, MA). Anti-CB2, antibody, GW3965 (for mouse treatment), T090 and SR144528 were supplied from Cayman Chemical (Ann Arbor, MI). H89 were from Calbiochem (San Diego, CA). Horseradish peroxidase-conjugated goat anti-rabbit and goat anti-mouse IgGs were obtained from Zymed Laboratories (San Francisco, CA). The solution of iron-NTA complex was prepared as described previously (Sakurai and Cederbaum, 1998).

2. Animal Treatments

Animal experiments were conducted according to the guidelines of the Institutional

Animal Use and Care Committee at Seoul National University. C57BL/6 mice (6-8 weeks of age) were purchased from Samtako Company (Osan, Korea). All the mice were acclimatized and kept at a temperature of 20 ± 2°C and a relative humidity of 50 ± 5% under filtered, pathogen-free air, with 12 h light/dark cycles, and food/water available ad libitum. CCl_4 (0.5 mL/kg, 1:20 in corn oil) was intraperitoneally injected to mice to induced acute (24 or 48 h) or chronic liver injury (twice a week for 4 weeks). For experiments testing the effects of GW3965 (LXRα agonist) on liver injury, mice were orally administered with GW3965 (10 mg/kg/day) for 3 days as described previously. 6 h after the last administration of GW3965, the mice were injected with CCl_4 and were killed after 24 h. For chronic CCl_4 injury model, LXRα$^{-/-}$ mice (purchased from the Jackson Laboratory) and their age-matched wild type control groups were injected with CCl_4 for 4 weeks. For hepatocyte specifically delivery of LXRα, the original EF1 promoter of pCDH-EF1-MCS-copGFP plasmid (System Biosciences) was replaced with the albumin enhancer/promoter (kindly provided by Dr. Richard D. Palmiter from University of Washington) (Pinkert et al., 1987). The coding region of pCMV-LXRα (kindly provided Dr. Mi-Ock Lee from Seoul National University) was extracted and cloned downstream of the albumin enhancer/promoter. $1.3x10^5$ viruses in 200 μL PBS per mouse were administered to 8-week-old LXRα$^{-/-}$ mice via tail vein. One week after the lentiviral delivery, the mice were treated with CCl_4 twice a week for 4 weeks and were sacrificed 24 h afterward. In experiments of

testing the liver protective effects of MB, MB was administered to mice (3 mg/kg/day, p.o.) for 3 days. 6 h after the last MB administration, mice were injected with CCl_4 for 48 h and were killed thereafter (Wu et al., 2014).

3. Histopathology and Blood Biochemical Analysis

Hematoxylin & Eosin (H&E) staining was performed as previously described (Han et al., 2016), the left lateral lobe of the liver was sliced, and the slices were fixed in formalin for 6 h. Then, the fixed samples were embedded in paraffin, and were cut into thick sections (4 μm), and stained with H&E. TUNEL assay was done using the DeadEnd Colorimetric TUNEL System (Promega, Madison, WI), as previously described (Han et al., 2016). Liver tissues or AML12 cells were fixed with formalin and were permeabilized with Triton X-100. Then the sample was incubated with biotinylated nucleotide and terminal deoxynucleotidyl transferase, followed by immersing in saline sodium citrate buffer. Endogenous peroxidases were blocked by using H_2O_2, followed by horseradish peroxidase-labeled streptavidin solution. Toward the end, the samples were developed using H_2O_2 and diaminobenzidine, and were examined with a light microscope. TUNEL-positive cells counting were repeated three times. Serum alanine aminotransferase (ALT) and aspartate aminotransferase (AST) activities were analyzed using Spectrum from Abbott Laboratories (Abbott Park, IL). Serum TNFα and IL1β were analyzed using commercial ELISA kit (Thermo Science, Rockford, IL) (Enzo Life, Farmingdale, NY). Briefly, serum (50 μl each) was loaded in the anti-mouse pre-coated

microtiter plate, and were incubated with biotinylated anti-TNFα (or IL1β) antibodies, followed by adding streptavidin conjugated to horseradish peroxidase. The color was developed using tetramethylbenzidine. Intensity of the color was measured at 450 nm by using a microplate reader (Tecan, Research Triangle Park, NC).

4. Cell Culture

Primary hepatocytes were isolated and incubated, as previously described (Wu et al., 2014). Briefly, mice were anesthetized with Zoletil, liver was perfused with Ca^{2+}-free Hank's buffered salt solution (Invitrogen, Carlsbad, CA), and was continuously perfused with 0.1% w/v collagenase (Sigma, Type IV). Then cut off the liver and washed with PBS. Liver cells were filtered with strainer (70 μm). Primary hepatocytes were plated in collagen-coated plates (5×10^5 cells/well) in dulbecco's modified eagle's medium (DMEM) containing 10% fetal bovine serum (FBS) and antibiotics (50 units/mL penicillin and 50 μg/mL streptomycin). AML12 cells (a mouse hepatocyte-derived cell line with typical hepatocyte features) and HepG2 cells (a human hepatocyte-derived cell line) were purchased from American type culture collection (ATCC, Rockville, MD). AML12 cells were cultured in the DMEM/F-12 containing 10% FBS, insulin-transferrin-selenium X, dexamethasone (40 ng/mL) and antibiotics. HepG2 cells were maintained in the DMEM containing 10% FBS and antibiotics. The cells were plated in six-well plate (2×10^5 cells/well) and were used when confluency reached 70-80%.

5. Bioinformatic Studies

For hierarchical cluster analysis, microarray data were supplied from the Gene Expression Omnibus (GSE25583) (Marquardt et al., 2012). Differentially expressed genes (DEGs) with statistical significance ($P<0.1$) in the livers of CCl_4-treated mice compared to those of vehicle-treated controls were selected. Heatmap was draw with R software (Bioconductor, pvclust). Genes encompassing 1% DEG which includes LXRα were selected and further categorized according to gene ontology terms using DAVID 6.7 software (Huang da et al., 2009). For gene interaction network analysis, DEGs with statistical significance ($P<0.05$ with fold change over 2) in LXR knockout mice compared to that of wild type mice in GEO data set (GSE38083) (Ducheix et al., 2013) were selected. Clustered DEGs were ranked according to KEGG pathway using DAVID 6.7 Software. Gene network of upregulated DEGs was extracted using Mentha and Cytoscape 3.0.0 software.

6. Immunoblot Analysis

Immunoblot analysis was performed as described previously (Wu et al., 2014). Cell lysates (or liver homogenates) were centrifuged to get supernatants (10,000 g, 10 min). Protein concentrations of each sample were measured by spectrophotometer (GE Healthcare, Biochrom Ltd, Cambridge, UK). Samples were equally made to a same concentration. Protein samples were loaded in gel electrophoresis, and were transferred to nitrocellulose membrane. The membrane was incubated with first antibodies of

interest, followed by incubating with HRP-conjugated secondary antibodies. Protein bands were developed using ECL system from Amersham (Chalfont St. Giles, Buckinghamshire, UK).

7. Reverse Transcription and quantitative RT-PCR assays

Experimental details are described elsewhere (Heo et al., 2014). Total RNA was isolated with Trizol reagent (Invitrogen, Carlsbad, CA), and was reverse-transcribed to obtain cDNAs. cDNAs were amplified by polymerase chain reaction (PCR) using the PCR Master kit (Roche, Mannheim, Germany). Quantitative real-time PCR (qRT-PCR) was performed using ABI StepOne plus Real-Time PCR System (Thermo Fisher Scientific) and SYBR Premix Ex Taq II kit (Takara Bio, Shiga, Japan). The relative levels of mRNA were normalized by actin. For qRT-PCR assays of miRNA, cDNAs were generated from total RNA (1 μg/per sample) using the miScript Reverse Transcription kit (Qiagen GmbH, Hilden, Germany). The levels of U6 small RNA were quantified for normalization of miRNA levels. The primers used in the qRT-PCR assays are listed in Table 1.

Gene symbol	Forward sequence	Reverse sequence
Mouse mRNA		
Lxrα	TGCCATCAGCATCTTCTCTG	GGCTCACCAGCTTCATTAGC
Cb2	GGTCGACTCCAACGCTATCTTC	GTAGCGGTCAACAGCGGTTAG
Dhcr24	CTGCCTACGAGCTGATCCTG	GTACAGCAACCCTTCCACGA
As3mt	TCTGCCACATTTCGCCTCTT	ATCCGGAGCAAAACGTGAGT
Acads	TTGCCGAGAAGGAGTTGGTC	AGGTAATCCAAGCCTGCACC
Tek	TCGGCTGGAATGACTTGCAT	CCAAAGTTGCCCTCTCCGAT
F5	CCGAGAGGAAGGATGATGCC	AAGCAGAGGCCCAATCAGAC
Actin	CTGAGAGGGAAATCGTGC	TGTTGGCATAGAGGTCCT
Tgfβ	CTTCAGCTCCACAGAGAAGAACTGC	CACAATCATGTTGGACAACTGCTCC
Tnfα	TACTGAACTTCGGGGTGATCGGTCC	CAGCCTTGTCCCTTGAAGAGAACC
iNOS	CCTCCTCCACCCTACCAAGT	CACCCAAAGTGCTTCAGTCA
Il6	TTCCATCCAGTTGCCTTCTT	ATTTCCACGATTTCCCAGAG
miRNA		
miR-27b	TTCACAGTGGCTAAGTCTGC	Universal reverse primer (Qiagen proprietary information)
let-7g	TGAGGTAGTAGTTTGTACAGTT	
miR-15a	TAGCAGCACATAATGGTTTGTG	
miR-185	TGGAGAGAAAGGCAGTTCCTGA	
miR-429	TAATACTGTCTGGTAATGCCGT	
ChIP primers		
LXRE1	ATGAGGAAGATACAATACCAGAGTATG	AAGACAAGGTTTCTCTGTAGCC
LXRE2	CAGGAGATCCGAAGCCTCTT	CTAGGCTGGCTGTCTCCATC
LXRE3	AGATGGAGACAGCCAGCCTA	AGACACCATTCCACACAGCA

Table 1. Primer sequences

8. Flow Cytometric Analysis

Flow cytometric analysis for apoptosis and H_2O_2 detection were done according to previous published method (Wu et al., 2014; Yang et al., 2015). Cells were detached by trypsinization and washed with PBS (1% FBS contained), followed by staining with FITC-Annexin V and propidium iodide (PI) for apoptosis analysis (or stained with 10 μM DCFH-DA for H_2O_2 detection). Fluorescence intensity was detected by a flow cytometer (BD Biosciences, San Jose, CA). 5,000 (apoptosis) or 10,000 (H_2O_2) gated events were recorded in each sample.

9. Chromatin immunoprecipitation (ChIP) Assays

ChIP assay was performed according to the kit protocol (Upstate Biotechnology, Lake Placid, NY), as described elsewhere (Han et al, 2016). After treatment of cells, formaldehyde was added to cross-link DNA and protein. PCR was done using the primers for LXRE. 10% of cross-linked lysates were used as input. The primers used in the PCR assays are listed in Table 1.

10. Reporter Assays

For luciferase assays, the region containing -1400 bp of the mouse *Cb2* gene was cloned into the pGL3 luciferase vector (pGL3-CB2). A mutation of LXRE was done by deleting the sequence of LXRE2 binding element. AML12 cells were transfected with pGL3-CB2 or pGL3-CB2 mutant with LXRE2 deletion (pGL3-CB2-LXRE2 del), and luciferase activity was measured (Promega, Madison, WI). For USP4-3′UTR reporter

assays, the miRNA 3'UTR target clone (Luc-USP4-3'UTR) containing firefly luciferase and renilla luciferase (an internal control) was commercially from GeneCopoeia (Product ID: HmiT055448-MT01, Rockville, MD). The Luc-USP4-3'UTR clone and miR-27b mimic (or ASO) were co-transfected FuGENE® HD Reagent (Roche, Indianapolis, IN). The activities of Firefly and renilla luciferase were measured sequentially using Luc-Pair miR Luciferase Assay kit according to the protocols (GeneCopoeia, Rockville, MD). Luciferase activities were normalized to those of Renilla luciferase.

11. Immunoprecipitation

Immunoprecipitation was done according to previous report (Kang et al., 2012). AML12 cells were transfected with His-tagged ubiquitin. After treatment, cell lysates were incubated with antibody against TβRI antibody (4°C for overnight). The antigen-antibody complex was pulled down by protein G-agarose (4°C for 2 h), followed by solubilizing in 2× Laemmli buffer and boiling for 5 min. The immunoprecipitation were resolved by SDS-PAGE and were developed with antibodies against ubiquitin or TβRI.

12. Plasmid, miRNA mimic, miRNA ASO and siRNA transfection

Flag-tagged-USP4 was purchased from Origene (RC224586, Rockville, MD) and Myc-tagged DN-AMPK was a gift from Dr J. Ha (Kyung Hee University, Korea). MiR-27b mimic (sense: 5'-UUCACAGUGGCUAAGUUCUGC-3', antisense: 5'-AGAACUUAGCCACUGUGAAUU-3') or miR-27b ASO (5'-

GCAGAACTTAGCCACTGTGAA-3') were used for miR-27b modulation. The scrambled control mimic (sense: 5'-GCAAUUUGGCGUCCUCCACUAA-3', antisense: 5'-AGUGGAGGACGCCAAAUUCCCU-3') or control ASO (5'-CCTTCCCTGAAGGTTCCTCCTT-3') were used for mock transfection. All nucleotides were 2'-*O*-methyl modified. Plasmid transfection (100 nM) was done using FuGENE® HD Reagent (Roche, Indianapolis, IN). For siRNA transfection, cells were transfected with siControl or siPKA (or siLKB1) (Santa Cruz, CA) using AMAXA nucleofection system (Lonza, Köln, Germany).

13. PKA Activity

PKA activity was done using a commercial kit from Enzo Life Sciences (Farmingdale, NY). 30 μg samples were loaded in the microtiter plate, followed by ATP addition (10 μg). Antibody against phosphorylated substrate was added after termination of the kinase reaction, followed by binding with peroxidase-conjugated secondary antibody. The color was developed using tetramethylbenzidine substrate, and reaction was stopped by adding acid stop solution. Intensity of the color was measured at 450 nm by using a microplate reader (Tecan, Durham, NC).

14. MTT Assay

MTT assay was used to measure cell viability as described previously (Wu et al., 2014). HepG2 cells were plated and incubated in a 48-well plate. After drug treatment, MTT was added to stain living cells (0.25 mg/mL, 0.25-1 h). The culture media were

removed, and DMSO (200 μL) were added to produce formazan crystals. Absorbance was measured (540 nm) using a microplate reader (Tecan, Research Triangle Park, NC). The viability of cells was defined by normalizing to untreated control.

15. Determination of GSH content

Cellular GSH content was determined using a commercial kit (Oxis International, Portland, OR), and GSH content was measured as described previously (Choi et al., 2010).

16. Data Analysis

For animal experiment and cell-based assays, data represent the mean ± SEM. Statistical significance was calculated using Student's t-test or one-way analysis of variance (ANOVA) test for multiple comparisons. Coefficients of correlation (r) were determined by the Pearson analysis. Statistical calculations of Pearson's correlation were performed using SPSS 22.0. P values of <0.05 were considered significantly different.

III. Results

1. PKA-GSK3β pathway for hepatocyte survival

1.1 PKA-dependent LKB1 activation by MB and AMPK activation

MB prevents ROS formation by combining electron leaked from mitochondrial electron transport (Atamna et al., 2008). LKB1 mediated AMPK activation plays important roles in maintaining energy homeostasis (Jeon et al., 2012; Shaw et al., 2005). Many antioxidants (e.g., metformin, polyphenols and flavonoids) can activate LKB1-AMPK and consequently protect hepatocytes from injury (Shaw et al., 2005; Kim et al., 2012; Choi et al., 2010). Therefore, whether MB can also activate the LKB1-AMPK signaling was measured. MB increased the phosphorylation LKB1 time-dependently (Fig. 1A). Since PKA may phosphorylate and activate LKB1 (Collins et al., 2000), whether knockdown of PKA in HepG2 cells can block MB-mediated LKB1 phosphorylation was examined. siPKA knockdown totally prevented MB to phosphorylate LKB1 (Fig. 1B). The results here suggest that PKA is required for LKB1 activation by MB.

Next, AMPK phosphorylation was examined. MB treatment enhanced both AMPK and its substrate, acetyl-coA carboxylase (ACC) phosphorylation notably (Fig. 1C). Moreover, the ability of MB to activate AMPK was eliminated upon LKB1 knockdown or in LKB1 deficient HeLa cells (Fig. 1D). Collectively, these results indicate that MB can activate AMPK via LKB1, which is downstream from PKA.

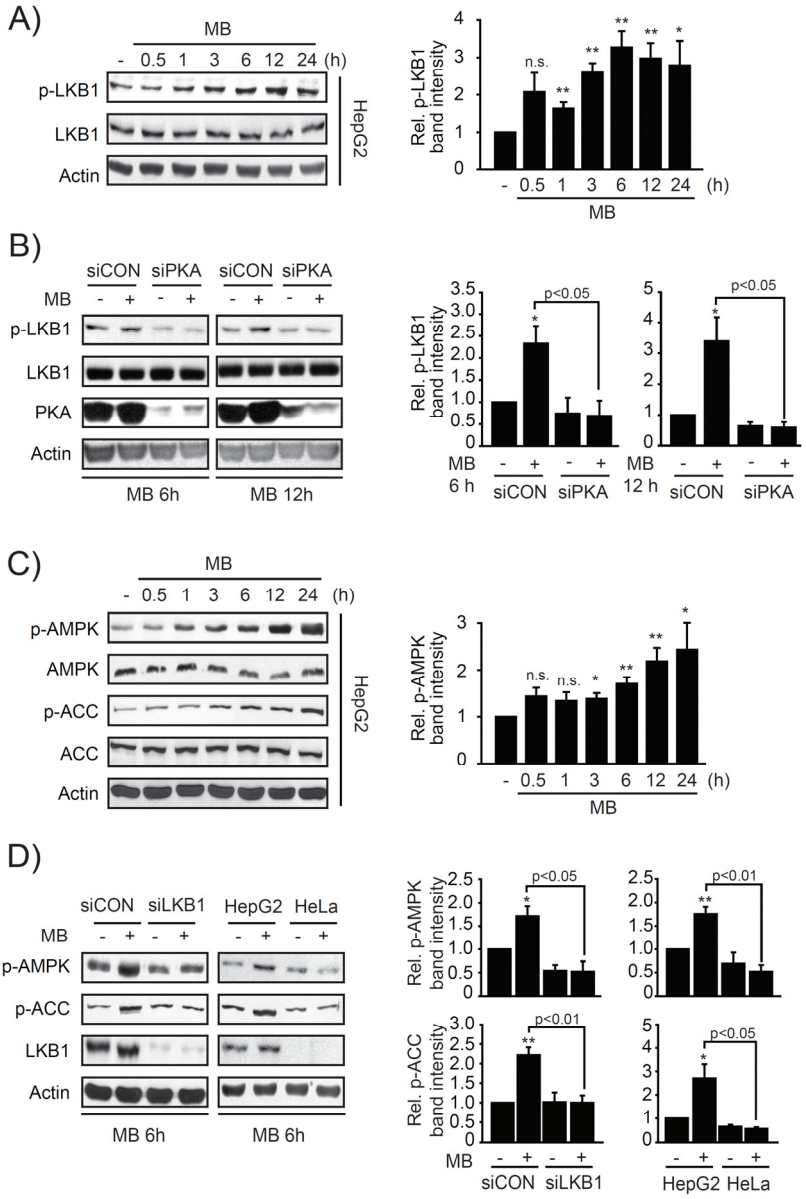

Figure 1. MB activates LKB1-AMPK, downstream of PKA

(A) Immunoblottings of LKB1 phosphorylation were done on the lysates of HepG2 cells treated with 1 μM MB in a time-dependent manner.

(B) HepG2 cells were incubated with 1 μM MB in a time-dependent manner as indicated after siRNA transfection for PKA (or control) (100 nM, 48 h). Protein levels of phosphorylated (or total) LKB1 and PKA were measured.

(C) Immunoblottings for phosphorylated (or total) AMPK and ACC were done on the cell lysates treated as in panel A.

(D) Left panel: HepG2 cells were treated with 1 μM MB for 6 h after siLKB1 or siCON transfection (100 nM, 48 h). Right panel: HepG2 or the LKB1 deficient HeLa cells were treated with 1 μM MB for 6 h. Immunoblottings for protein levels were measured on the cell lysates.

Data represent the mean ± SEM of at least three separate experiments. Significantly different as compared with experimental control: *P<0.05, **P<0.01, n.s., not significant.

1.2 Dual regulation of GSK3β downstream of PKA

AMPK activation has been shown to protect mitochondria and contribute to cell viability via GSK3β inhibition (Choi et al., 2010). Therefore, whether MB facilitated GSK3β inhibition was assessed. As a result, MB treatment enhanced GSK3β phosphorylation at S9 (inhibitory phosphorylation) and decreased GSK3β phosphorylation at Y216 (active phosphorylation) (Fig. 2A). Accordingly, the activity of GSK3β, reflected by the ratio of Tyr/Ser GSK3β, decreased throughout the time of MB treatment.

According to the results, the S9 phosphorylation of GSK3β occurred at around 30 min, which is earlier than LKB1 and AMPK phosphorylation (1 h and 3 h, respectively). Moreover, functional inactivation of AMPK could not block the upregulation of S9-GSK3β S9 at 1 h MB treatment, where it did so at 12 h (Fig. 2B), suggesting that increased S9-GSK3β at early time (30 min-1 h) by MB is not mediated by AMPK, whereas the later time (6 h-24 h) may depend on AMPK. We determined whether PKA is responsible for the molecular event, since PKA can inhibit GSK3β via S9 phosphorylation (Fang et al., 2000). As expected, siPKA transfection or PKA inhibitor H89 pretreatment completely blocked GSK3β S9 phosphorylation by MB after 1 h treatment (Fig. 2C), indicating that PKA is the kinase responsible for GSK3β S9 phosphorylation at early time (i.e. 0.5-1 h), and LKB1-AMPK controls GSK3β S9 phosphorylation at later time (6-24 h), which is also derived from PKA.

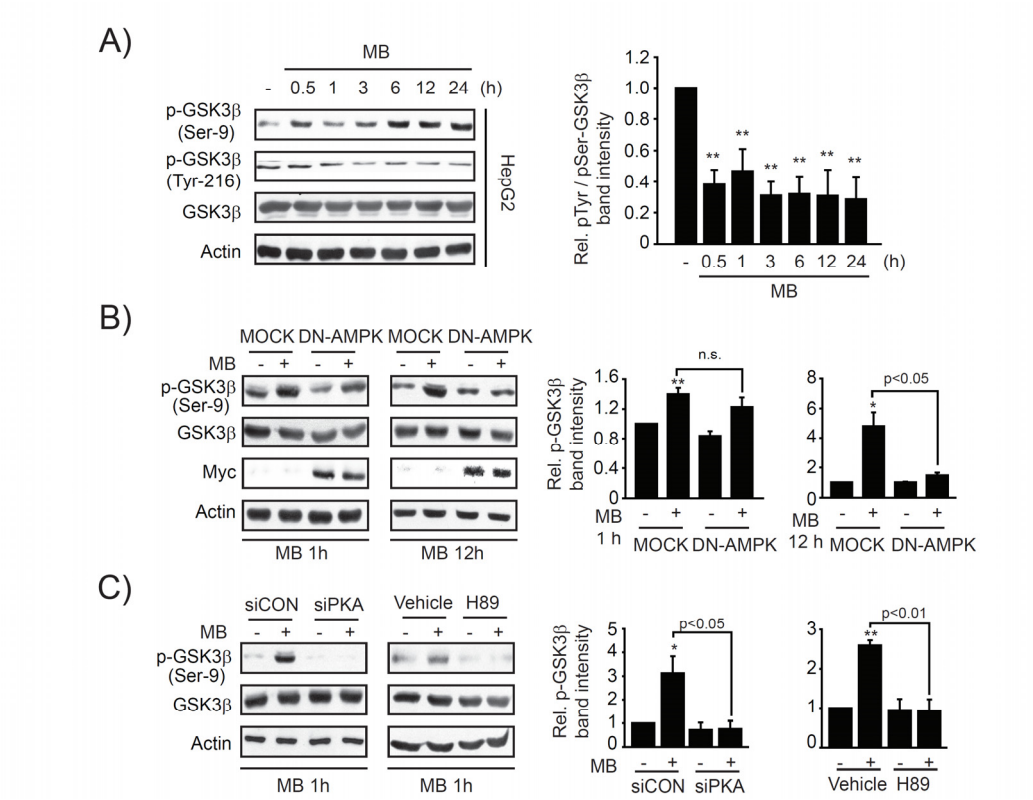

Figure 2. MB inhibits GSK3β activity

(A) Immunoblottings were done on HepG2 cell lysates treated with 1 μM MB as indicated.

(B) Cells were treated with MB (1 μM, for 1 or 12 h) after DN-AMPK transfection.

(C) HepG2 cells were treated with MB (1 μM for 1 h) after indicated siRNAs transfection (100 nM, 48 h) or 1 μM H89 pretreatment for 30 min.

Data represent the mean ± SEM of three or four separate experiments. Significantly different as compared with experimental control: *P<0.05, **P<0.01, n.s., not significant.

2. LXRα-associated pathway for hepatocyte survival and involvement of PKA

2.1 The impact of LXRα on hepatocyte protection

To understand the role of LXRs in liver injury, gene expression omnibus (GEO) database was used to analyze the mRNA levels of *LXRα* and *LXRβ* in several liver injury models. These liver injury models include toxicant challenged human primary hepatocytes or mouse liver (GSE13430, GSE17184), and very early HCC or cirrhosis conditions in human liver (GSE6764, GSE25097). Our data showed that *LXRα* significantly decreased in different liver damage conditions (Fig. 3A). As a contrast, the level of *LXRβ* was not significantly changed (Fig. 3A).

To characterize whether LXRα activation protect against toxic liver injury, the effects of GW3965 (LXRα agonist) on acute CCl_4 induced liver damage in mice were measured. TUNEL staining showed pretreatment of GW3965 decreased hepatocyte apoptosis induced by CCl_4 (Fig. 3B left). CCl_4 induced alternations in apoptosis/survival markers (cleaved-caspase 3, cleaved-PARP and pAKT) were all blunted by GW3965 (Fig. 3B right), confirming the liver-protective effects of LXRα activation. Next, LXRα knockout mice ($LXR\alpha^{-/-}$) were applied to specify the role of LXRα in hepatocyte protection. $LXR\alpha^{-/-}$ mice showed exacerbated hepatocyte apoptosis and injury as evidenced from TUNEL, H&E staining and apoptosis/survival markers alternations (Fig. 3C), suggesting LXRα absence exacerbates hepatocyte injury. These data suggest that LXRα expression is a determinant for protecting hepatocyte and liver.

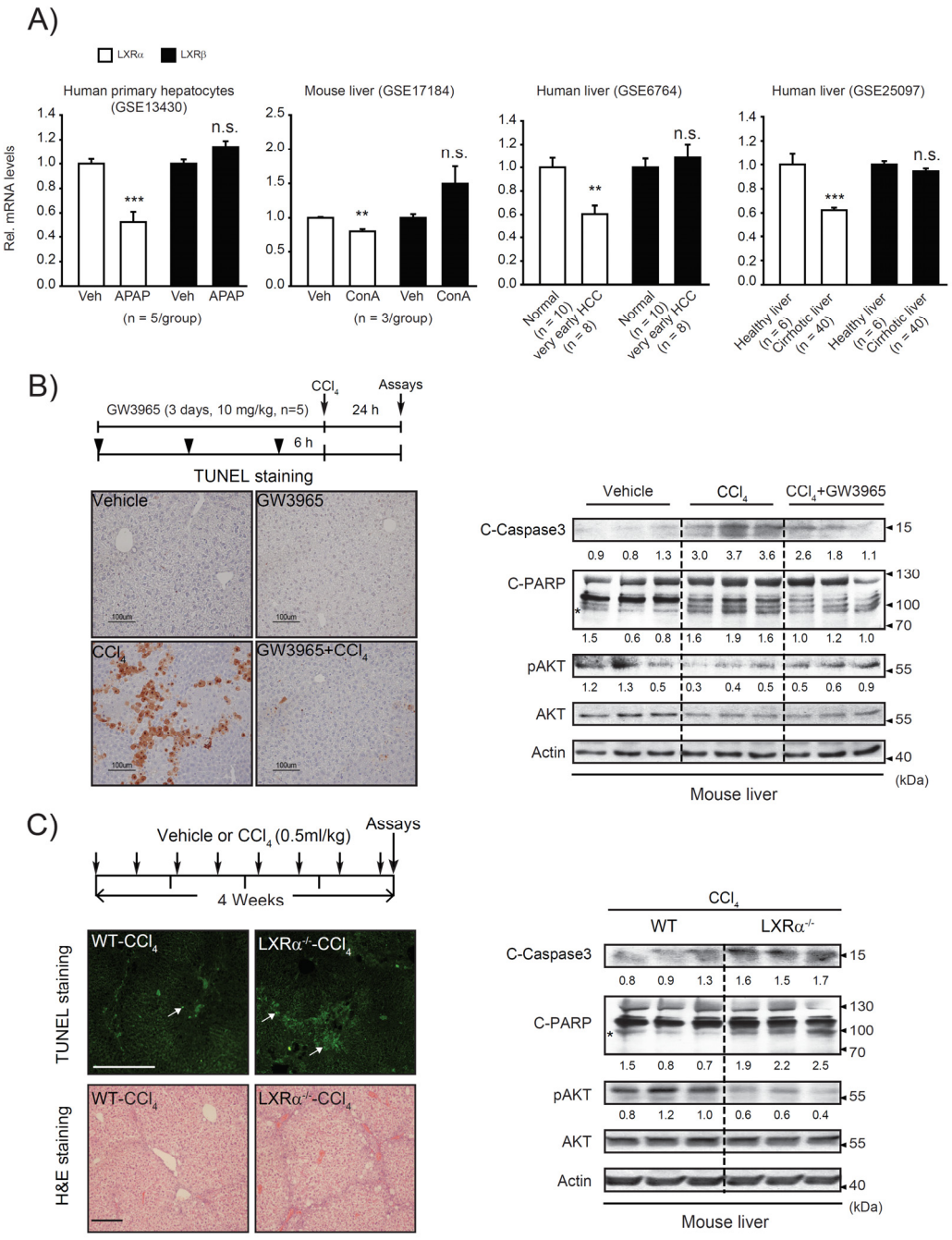

Figure 3. LXRα protects hepatocytes against toxicant induced injury

(A) mRNA levels of *LXRα* and *LXRβ* were analysed by using several liver injury related GEO database (GSE13430, GSE17184, GSE6764 and GSE25097). Data represent the mean ± SEM. Significantly different as compared with experimental control: **P<0.01; ***P<0.001. n.s., not significant; Veh, vehicle; APAP, acetaminophen; ConA, concanavalin A.

(B) Mice (n = 5/group) were orally administered with GW3965 (10 mg/kg/day) for 3 days and were injected with CCl_4. Mice were sacrificed 24 h thereafter. Apoptotic hepatocytes were detected by TUNEL staining of the liver sections (left panel; scale bar = 100 μm) and liver protein levels of death/survival markers were measured (right panel).

(C) WT and LXRα$^{-/-}$ mice were intraperitoneally injected with CCl_4 for 4 weeks (n = 5/group). TUNEL and H&E stainings (scale bar = 100 μm) were done on liver tissue and liver protein levels of death/survival markers were measured.

For B-C, values below blots represent relative fold change compared with experimental control; quantification is normalized to actin (loading control).

2.2 LXRα protection of hepatocytes against TGFβ-induced apoptosis

Above results have demonstrated that activation of LXRα protects liver against toxicant induced hepatocyte death and injury. In addition, knockdown of LXRα amplifies the levels of hepatocyte death and liver injury. In the following study, the research aim focused on the molecular mechanism by which LXRα exerts its protective effects on hepatocyte. To investigate the underlying molecular basis of hepatocyte protection by LXRα, we used a GEO database studying the altered expression of liver genes upon LXR knockdown (GSE38083). The hepatic gene expression profiles in LXR knockout mice were analyzed and DEGs ($P<0.05$ with fold change over 2 or under 0.5) were extracted in LXR knockout mice comparing to wild type mice. The upregulated DEGs were then subjected into the pathway analysis using KEGG database. As a result, the pathways related with cytotoxicity (e.g., “natural killer cell mediated cytotoxicity”), drug metabolism (e.g., “drug metabolism-cytochrome P450” and “metabolism of xenobiotics by cytochrome P450”) and inflammation (e.g., “chemokine signaling”) were enriched in the upregulated DEGs (Fig. 4 left). The DEGs increased in $LXR^{-/-}$ mice liver were further subjected to gene network analysis. According to the gene network, TGFβ signaling (TGFBR1 and TGFBR2) appeared to be a bridge in the core network (Fig. 4 right). Giving the known fact that TGFβ is associated with ROS production and promotes hepatocyte apoptosis (Black et al., 2007), the results suggest that the cytoprotective role of LXRα may be involved in inhibition of TGFβ signaling.

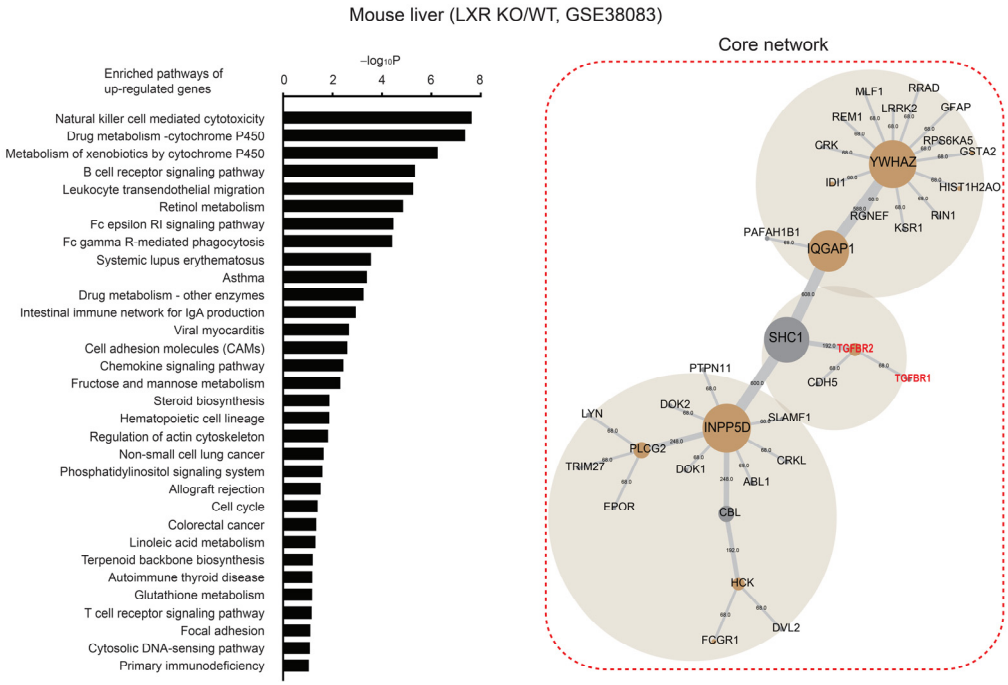

Figure 4. LXRα antagonizes TGFβ signaling

A GEO database (GSE38083) of LXR knockout mice liver comparing to wild type mice liver was selected for analysis. Upregulated DEGs were extracted according to specific fold change or P value as described in the material and methods. Metabolic pathways analysis of upregulated DEGs was done using KEGG database (left panel). Gene interaction network was obtained by using Mentha software and Cytoscape 3.0.0 software (right panel).

Giving the predicted antagonistic relationship between LXRα and TGFβ, we next examined whether GW3965 can inhibit TGFβ signaling. As expected, GW3965 attenuated TGFβ-induced phosphorylation on Smad2 and Smad3 (Fig. 5A), corroborating the possibility of LXRα to inhibit TGFβ signaling. Treatment of AML12 cell with TGFβ significantly induced apoptosis according to TUNEL staining results, and the apoptosis was decreased by GW3965 pretreatment (Fig. 5B). Besides, the cytoprotective effect of GW3965 was also verified by FACS analysis of FITC-Annexin V/PI fluorescence. At 24 h after TGFβ treatment, up to 21.7% (Annexin V^+/PI^-) and 8.2% (Annexin V^+/PI^+) of AML12 cells underwent early and late apoptosis respectively, while GW3965 pretreatment attenuated the populations of both early and late apoptotic cells (Fig. 5C), indicative of LXRα activation rescue of the hepatocytes from death. In addition, TGFβ-induced the alternations of apoptotic/survival protein markers were reversed by GW3965 in both mouse primary hepatocytes and AML12 cells (Fig. 5D). Moreover, apoptosis marker cleaved-caspase 3 was more significantly increased by TGFβ in LXR$\alpha^{-/-}$ mouse primary hepatocytes comparing to that of WT mice, indicating a susceptibility of LXRα to the level of TGFβ (Fig. 5E). These results confirmed the antagonistic relationship between LXRα and TGFβ by demonstrating that LXRα activation protects hepatocytes from TGFβ-induced death, and LXRα is required for maintaining hepatocyte viability.

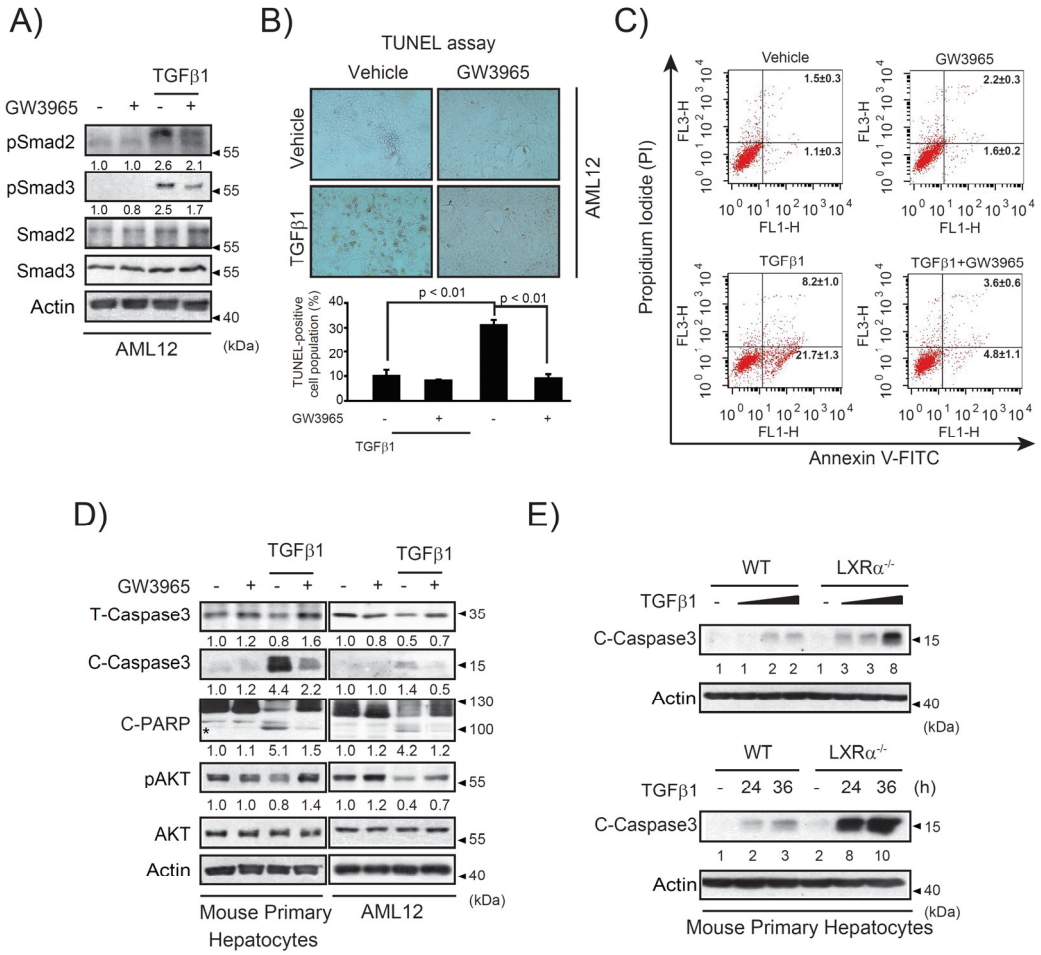

Figure 5. LXRα protects hepatocytes against TGFβ-induced apoptosis

(A) AML12 cells were treated with GW3965 (3 μM) for 1 h, followed by 30 min incubation of TGFβ (5 ng/mL). Protein levels of TGFβ downstream representative signaling markers, phosphorylations of Smad2 and Smad3, were measured by immunoblotings.

(B) AML12 cells were treated with 3 μM GW3965 for 1 h, followed by incubating with 5 ng/mL TGFβ for 24 h and TUNEL assay was carried out. TUNEL-positive cells were counted and data represent the mean ± SEM of three replicates.

(C) AML12 cells were treated as described in panel B. Cells were then subjected to FITC-Annexin V/PI staining and fluorescence were measured by flow cytometry. Values represent three separate experiments.

(D) Mouse primary hepatocytes or AML12 cells were treated as described in panel B. Protein levels of apoptosis/survival markers were measured by immunoblottings.

(E) Primary hepatocytes were isolated from wild type or LXR$\alpha^{-/-}$ mice, and were exposed to TGFβ (0.05 ng/mL, 0.5 ng/mL or 5 ng/mL) for 24 h (upper panel) or with 5 ng/mL TGFβ for 24 or 36 h (lower panel). Protein levels of cleaved-caspase 3 were measured.

For A, D and E, values below blots represent relative fold change compared with experimental control; quantification is normalized to actin (loading control).

2.3 Positive correlation between LXRα and CB2 in liver injury conditions

Having identified the hepatocyte protective effects of LXRα, we next investigated which downstream molecule(s) might be responsible for the effects shown by LXRα. Through analyzing the mouse gene expression database (GSE25583) of CCl_4 administrated-mice liver, hepatic gene expression patterns in mice with or without CCl_4 treatment were clustered to place rows with similar response patterns near each other. The hierarchical cluster with closest expressional relevance to LXRα contained 21 genes, 7 of which (*Lxrα*, *As3mt*, *Acads*, *Tek*, *Cb2*, *F5* and *Dhcr24*) were identified as "response to stress/stimulus" term according to gene ontology analysis (Fig. 6A). To validate the prediction of microarray analysis in hepatocytes, the expression of these genes in mouse primary hepatocytes isolated from acute CCl_4-administrated liver were measured. Noticeably, mRNA levels of *Lxrα*, *Cb2* and *Dhcr24* in hepatocytes were significantly decreased in CCl_4 treatment group, whereas *As3mt*, *Acads*, *Tek* and *F5* showed no significant differences (Fig. 6B). As a result, *Lxrα* levels were highly correlated with *Cb2* (Fig. 6B). Consistently, the protein levels of LXRα and CB2 in hepatocytes were also decreased in CCl_4 treatment group with positive correlation (Fig. 6C). Moreover, the positive correlation of LXRα-CB2 can also be observed in both human and mouse hepatitis liver (GSE20140 and GSE17184) (Fig. 6D). Since *Dhcr24* is an established LXRα target gene (Wang et al., 2008), we then focused on investigating whether LXRα might regulate CB2.

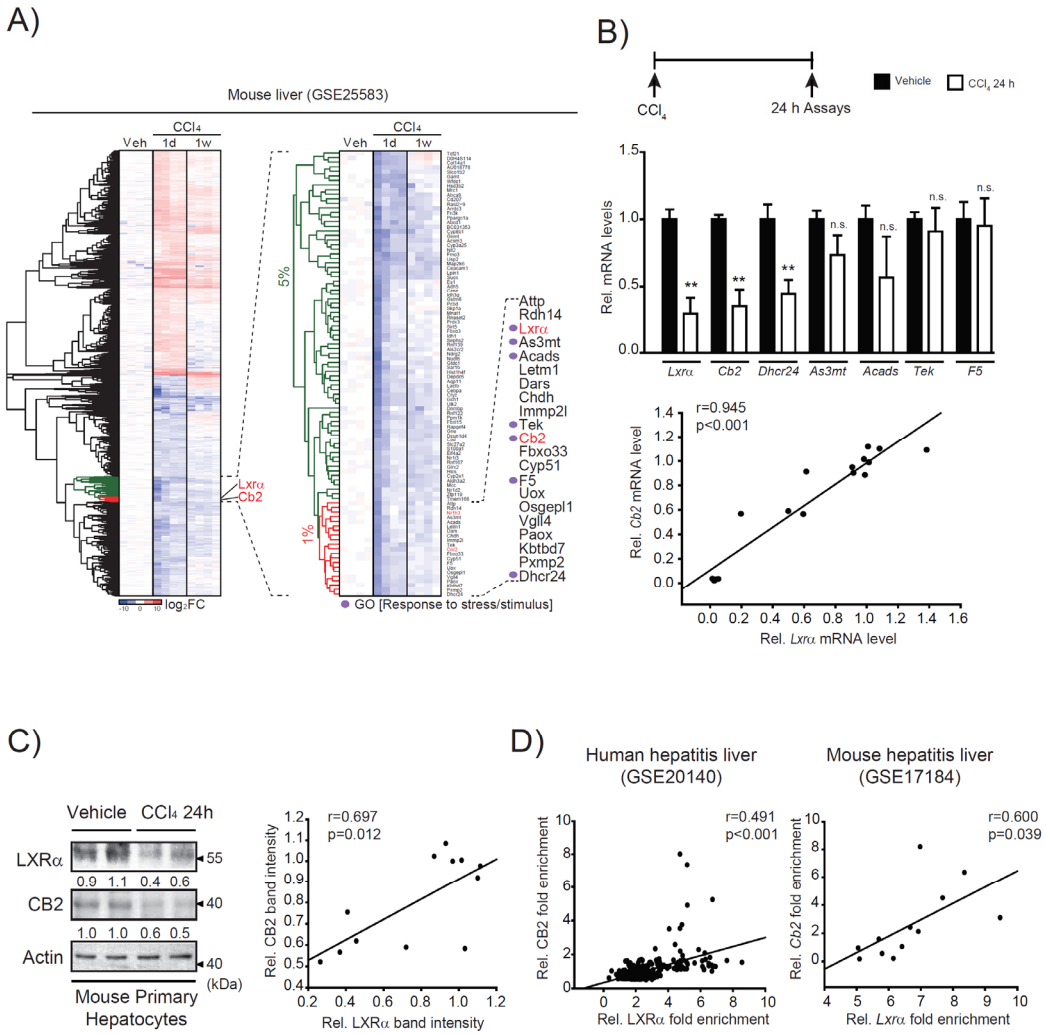

Figure 6. LXRα positively correlates with CB2 in liver injury conditions

(A) Heat map and hierarchical correlation analyses of the genes in the cDNA microarray obtained from GEO database (GSE25583). Genes' response patterns by CCl_4 compared with control group were presented using a heat map with hierarchical correlation (blue, downregulation; and red, upregulation). 1% LXRα-relevant genes were noted (purple

dots showing genes belong to “response to stress/stimulus” term upon gene ontology analysis).

(B) Mice were injected with vehicle or CCl_4 for 24 h (n = 4/group). Primary hepatocytes were isolated and *Lxrα* and relevant genes were measured by qRT-PCR assays. Correlation between *Lxrα* and *Cb2* were analysed. Coefficients of correlation were determined by the Pearson analysis. Data represent the mean ± SEM. Significantly different as compared with experimental control: **P<0.01. n.s., not significant.

(C) Protein levels were detected in mouse primary hepatocytes treated as in panel B. Correlation between LXRα and CB2 were analysed. Values below blots represent relative fold change compared with experimental control; quantification is normalized to actin (loading control).

(D) Correlations between *LXRα* and *CB2* in a large cohort of hepatitis patients (GSE20140) (n = 307) and mouse hepatitis liver (GSE17184) were determined. Coefficients of correlation were determined by the Pearson analysis.

2.4 LXRα transcriptional regulation of CB2

Since LXRα is ligand-activated receptor, the positive correlation between LXRα and CB2 in liver injury prompted us to determine whether a pharmacological activation of LXRα would have an inducible effect on CB2. To test the possibility *in vivo*, mice were orally administrated with GW3965, and CB2 levels were increased (Fig. 7A). Next, whether LXRα activation was able to increase CB2 expression in cell-based models were determined. In AML12 cells treated with GW3965, CB2 expression increased both in time and concentration-dependent manner (Fig. 7B). Consistently, another LXRα agonist T090 also enhanced CB2 protein level (Fig. 7B). Furthermore, GW3965 could also increase CB2 protein level in mouse primary liver cells, and this increase was abolished in primary hepatocytes from LXRα$^{-/-}$ mice, suggesting CB2 upregulation by GW3965 is LXRα-dependent (Fig. 7C). Moreover, overexpression of LXRα led an increased CB2 level in HEK293 cells (Fig. 7D). These results provide a possibility that LXRα activation may modulate CB2 expression both *in vitro* and *in vivo*.

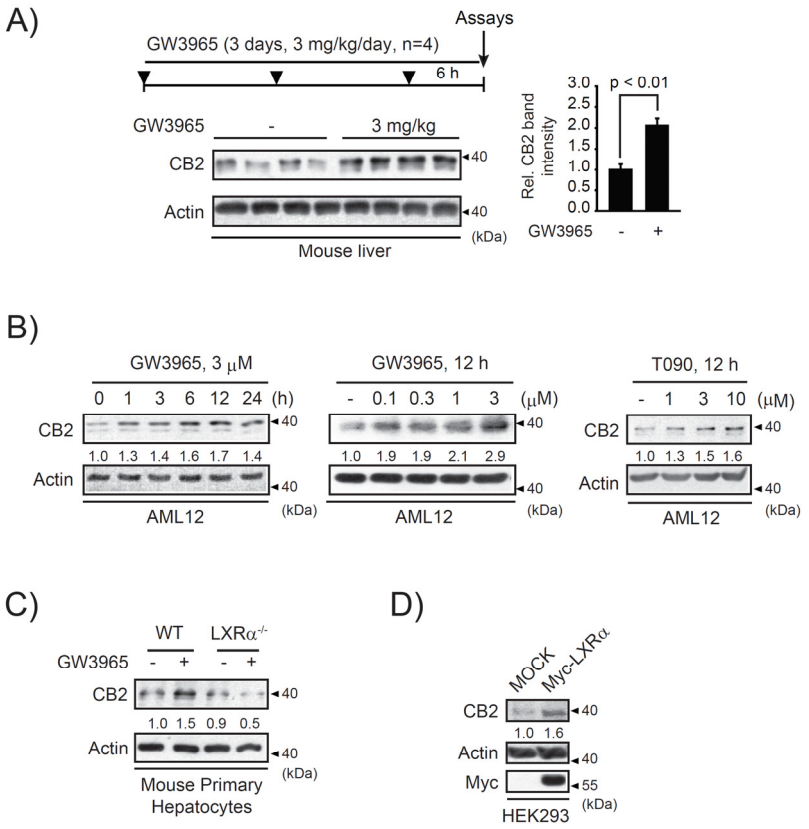

Figure 7. LXRα upregulates CB2 both *in vivo* and *in vitro*

(A) Hepatic CB2 levels were measured in GW3965-administered mice.

(B) AML12 cells were treated with LXRα agonists (GW3965 or T090) as indicated.

(C) CB2 immunoblottings in primary hepatocytes treated with GW3965 (3 μM, 24 h).

(D) HEK293 cells were transfected with the plasmid overexpressing Myc-LXRα or Mock (1 μg, 6 h). Protein levels of CB2 and Myc were detected on cell lysates.

For B-D, values below blots represent relative fold change compared with experimental control; quantification is normalized to actin (loading control).

Having identified the increased CB2 protein expression by activation of LXRα, we next wondered whether the increased protein level is associated with increased *Cb2* transcription. The *Cb2* mRNA levels in both *in vivo* and *in vitro* upon LXRα activation were measured. Experiment results showed that LXRα activation induced *Cb2* mRNA expression in both mouse liver and AML12 cells (Fig. 8A). LXRα is a transcription factor regulating target genes via transcriptionally regulation. So we hypothesized that LXRα may modulate CB2 expression via transcriptional regulation. Three putative LXRE motifs were found in *Cb2* gene promoter. To examine the physiologic occupancy of LXRα on the *Cb2* promoter, ChIP assay was performed. GW3965 induced LXRα occupancy at the -784 bp site (LXRE2) as verified by qPCR analysis (Fig. 8B). In addition, GW3965 significantly enhanced the luciferase activity of the reporter construct containing -1.4 kb mouse *Cb2* gene. However, transfection of a mutated vector with LXRE2 deletion abrogated the ability of GW3965 to trans-activate *Cb2* promoter activity (Fig. 8C). Together, these data demonstrate that LXRα transcriptionally controls *Cb2* gene expression.

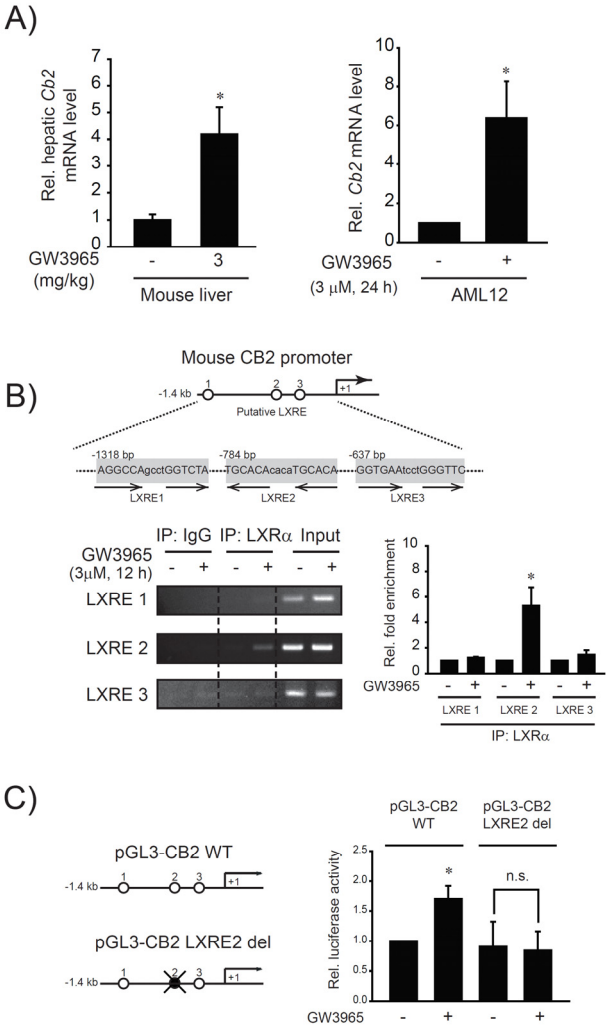

Figure 8. LXRα transcriptionally regulates CB2

(A) qRT-PCR assays of *Cb2* were done on GW3965-administered liver samples treated as in Fig. 7A (left panel) or in the GW3965 treated AML12 cells (3 μM, 24 h) (right panel).

(B) Three LXREs were found on the promoter of mouse *Cb2* gene. ChIP assays were performed as described in the materials and methods. LXRα and LXRE binding was verified by qPCR assays.

(C) The luciferase activity of CB2 gene promoter was measured in GW3965-treated AML12 cells following transfection with pGL3-CB2 construct or mutant construct with LXRE2 deletion (1 μg, 24 h).

For A-C, data represent the mean ± SEM of at least three separate experiments. Significantly different as compared with experimental control: *P<0.05, n.s., not significant.

Previous results have demonstrated a protective effect of LXRα on hepatocyte survival, as well as that LXRα regulates *Cb2* gene expression. Next, we wanted to explore that whether CB2 is involved in the cytoprotective effects of LXRα. CB2 has been reported have many beneficial effect on liver, such as preventing alcohol-mediated liver injury and fibrosis (Louvet et al., 2011; Muñoz-Luque et al., 2008). Whether CB2 can limit TGFβ mediated hepatocyte apoptosis has not been studied. In the current study, the effect of CB2 activation on TGFβ induced apoptosis was examined. Consequently, CB2 agonist JWH133 attenuated TGFβ induced cleaved-caspase 3 (Fig. 9A), suggesting CB2 protects hepatocytes against TGFβ induced apoptosis. Importantly, CB2 inverse agonist SR144528 reversed the effect of GW3965 against TGFβ (Fig. 9B), suggesting the requirement of CB2 for LXRα to protect hepatocytes. Our data strengthen the concept that LXRα activation, via CB2 induction, plays a critical role in antagonizing hepatocyte apoptosis to TGFβ stimulus.

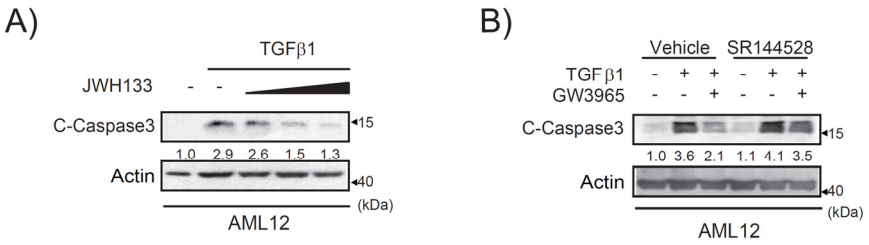

Figure 9. LXRα protection of hepatocytes is CB2-dependent

(A) AML12 cells were incubated with 1-10 μM JWH133 for 1 h, followed by TGFβ treatment for 24 h. Protein levels of apoptosis marker cleaved-caspase 3 were examined in the AML12 cell lysates.

(B) AML12 cells were incubated with SR144528 (4 μM, 30 min), and were treated with GW3965 (3 μM for 1 h), followed by exposure to TGFβ for 24 h. Cleaved-caspase 3 immunoblottings were measured.

Values below blots represent relative fold change compared with experimental control; quantification is normalized to actin (loading control).

2.5 Inhibition of USP4 and TβRI by LXRα and CB2

Having identified the LXRα-CB2 pathway for hepatocyte protection, attention was paid to the molecular basis downstream of CB2. Inhibition of TGFβ receptor 1 (TβRI) in hepatocytes diminished CCl_4 induced liver damage (Karkampouna et al., 2016), and ubiquitin modification of TβRI is a key mechanism of TGFβ signaling control (Aggarwal and Massagué, 2012). We examined whether LXRα facilitate TβRI ubiquitination. Immunoprecipitation indicated that LXRα activation enhanced TβRI ubiquitination in AML12 cells, and as a result attenuated protein level of TβRI in whole cell lysates (Fig. 10A). Moreover, treatment of the cells with GW3965 accelerated cycloheximide (CHX, a general protein synthesis inhibitor) mediated TβRI degradation, which can be blocked by CB2 inverse agonist SR144528 (Fig. 10B). These results demonstrate that LXRα repress TβRI protein stability through CB2.

It has been shown that USP4 amplifies TGFβ signaling by acting as a deubiquitylating enzyme and stabilizer for TβRI (Zhang et al., 2012). We next explored whether LXRα and CB2 could modulate the level of USP4. Protein level of USP4 decreased in GW3965 or JWH133 treated mouse primary hepatocytes (Fig. 10C). Of note, CB2 inverse agonist SR144528 blocked LXRα's repressive effect on USP4 (Fig. 10C), suggesting LXRα may negatively regulate USP4 through CB2. Furthermore, overexpression of USP4 attenuated GW3965's cytoprotective effects against TGFβ (Fig. 10D), supporting that LXRα may repress USP4-mediated TβRI through CB2.

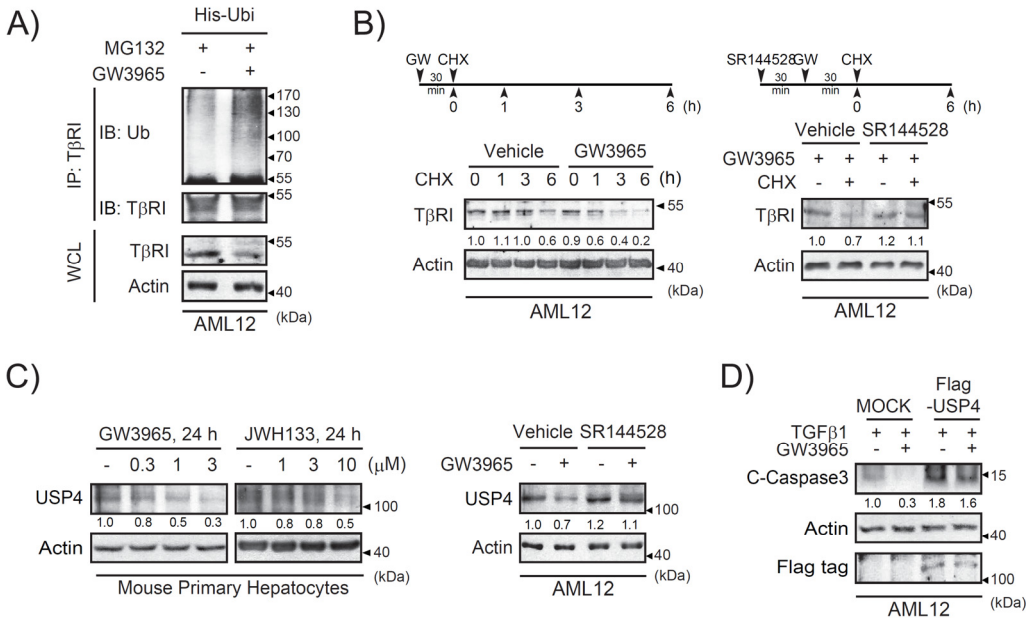

Figure 10. LXRα inhibits USP4-mediated TβRI stabilization via CB2

(A) AML12 cells were transfected with His-tagged ubiquitin (His-Ubi), followed by incubating 3 μM GW3965 for 24 h. MG132 (proteasome inhibitor, 10 μM) was added 6 h prior to lysis. TβRI protein complex were immunoprecipitated with anti-TβRI antibody and were immunoblotted with antibodies against ubiquitin or TβRI. Immunoblottings of TβRI and actin were measured in the whole cell lysates (WCL).

(B) Left panel: AML12 cells were incubated with CHX (protein synthesis inhibitor, 20 μg/mL) for the indicated times (0, 1, 3 and 6 h) with or without GW3965 pretreatment (3 μM, 30 min). Right panel: cells were incubated with SR144528 (4 μM, 30 min) and were treated with 3 μM GW3965 for 30 min, followed by CHX exposure for 6 h. TβRI was immunoblotted on the lysates.

(C) Immunoblottings for USP4 were measured on mouse primary hepatocytes treated with indicated concentration of GW3965 or JWH133 (left panel) for 24 h. AML12 cells were pretreated with SR144528 (4 μM, 30 min), followed by incubation of 3 μM GW3965 for 24 h (right panel).

(D) AML12 cells were transfected with Flag-tagged USP4 (1 μg, 24 h), and were exposed to TGFβ for 24 h with or without GW3965 pretreatment (3 μM, 1 h). Protein levels of cleaved-caspase 3 and flag-tag were measured in the cell lysates.

For B-D, values below blots represent relative fold change compared with experimental control; quantification is normalized to actin (loading control).

2.6 USP4 as a novel target of miR-27b

To investigate how LXRα-CB2 represses USP4, we determined whether it was through miRNA regulation. By comparing the 44 top decreased miRNAs in CCl_4 challenged mouse liver (Knabel et al., 2015) with candidate miRNAs that can potentially target to USP4 (microrna.org), a group of miRNAs were extracted (Fig. 11A). Among them, miR-27b was significantly increased by CB2 agonist JWH133 treatment (Fig. 11B). Moreover, CB2 inverse agonist SR144528 blocked the increased effect of LXRα agonist on miR-27b level (Fig. 11C), suggesting the possibility that LXRα increases miR-27b through CB2.

As a continuing effort to determine whether miR-27b inhibit USP4 by directly interacting with the 3'-UTR of USP4, the luciferase expression from Luc-USP4-3'-UTR construct after miR-27b mimic (or ASO) transfection was measured. MiR-27b mimic transfection decreased the luciferase activity, whereas miR-27b ASO transfection increased the luciferase activity (Fig. 11D). The effects of miR-27b modulation on USP4 protein levels were further assessed. As expected, transfection of miR-27b mimic repressed USP4 and miR-27b ASO had the opposite effect (Fig. 11E), suggesting that miR-27b has the ability to directly inhibit USP4. Further result showed CB2 mediated USP4 inhibition was attenuated by miR-27b ASO transfection (Fig. 11F), suggesting miR-27b contributes to CB2 mediated USP4 inhibition.

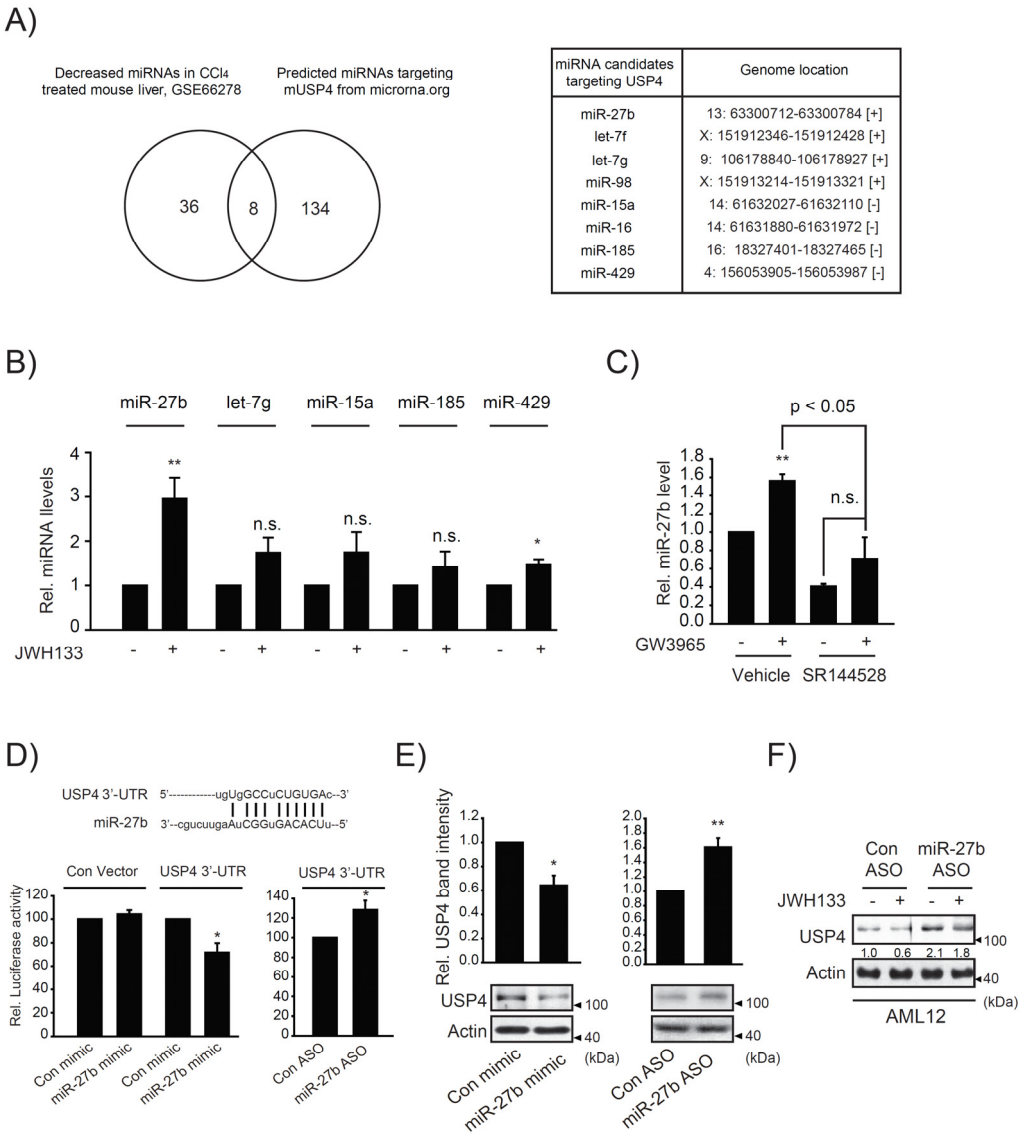

Figure 11. MiR-27b directly targets and inhibits USP4

(A) Left panel: an overlapping of top 44 decreased miRNAs identified in CCl_4 treated mouse liver (1 mL/kg, 8 weeks) (Knabel et al., 2015) and predicted miRNAs targeting

mouse USP4 (microRNA.org). Right panel: A list of overlapped miRNA candidates of two groups.

(B) AML12 cells were treated with 10 μM JWH133, the levels of miRNA candicates were examined by qRT-PCR assays.

(C) The level of miR-27b was determined by qRT-PCR assays in AML12 cells treated as in Fig. 10C right.

(D) Luciferase activity in AML12 cells co-transfected with miR-27b mimic (or ASO) and Luc-USP4-3'UTR construct.

(E) USP4 protein levels were examined in AML12 cells transfected with miR-27b mimic (or ASO).

(F) AML12 cells were transfected with miR-27b ASO for 48 h, and were treated with JWH 133 (10 μM, 24 h). Values below blots represent relative fold change compared with experimental control; quantification is normalized to actin (loading control).

For B-E, data represent the mean ± SEM of three separate experiments. Significantly different as compared with experimental control: *P<0.05; **P<0.01. n.s., not significant.

2.7 Role of PKA in LXRα associated signaling transduction

Next, we wondered the mechanism of miR-27b upregulation and USP4 repression by CB2 agonist. As a G-protein-coupled receptor, CB2 is catagorized into $G_{i/o}$-coupled receptors that are classically associated with decreased cAMP formation and consequent PKA inhibition. However, CB2 agonist JWH015 has been reported that can significantly increase cAMP (~10 fold) level from 2 h to 48 h (Börner et al., 2009), suggesting CB2 modulation on PKA activity is bifacial. In our study, GW3965 treatment raised basal PKA activity in AML12 cells (Fig. 12A), and CB2 agonist increased creb phosphorylation, an indicator of PKA activity (Fig. 12B). These data indicate that LXRα and CB2 may increase PKA activity. Moreover, whether PKA affect USP4 repression was determined. PKA inhibitor H89 blocked JWH133's ability in decreasing USP4 and TβRI (Fig. 12C), suggesting a requirement of PKA in the signaling transduction downstream of CB2. Consequently, the role of PKA in mediating LXRα's beneficial effect was examined. PKA knockdown reversed the cytoprotective effect of LXRα activation (Fig. 12D), suggestive of the critical role of PKA in mediating the survival signal downstream of LXRα and CB2.

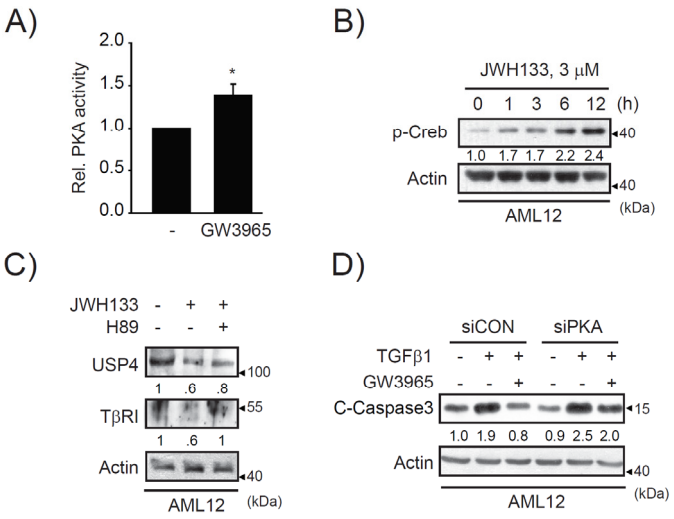

Figure 12. Involvement of PKA

(A) AML12 cells were treated with GW3965 (3 μM) for 3 h, and PKA activity was determined. Data represent the mean ± SEM of three separate experiments. Significantly different as compared with control: *P<0.05.

(B) AML12 cells were treated with 3 μM JWH133 for the indicated times, and immunoblotting for the phosphorylation of creb was measured in the cell lysates.

(C) AML12 cells were treated with H89 (1 μM, 30 min) followed by treatment of 10 μM JWH133 for 24 h, the immunoblottings for USP4 and TβRI were measured .

(D) AML12 cells were exposed to TGFβ for 24 h with or without 3 μM GW3965 pretreatment after siRNA for PKA or control transfection (100 nM, 48 h). Protein levels of cleaved-caspase 3 were measured.

For B-D, values below blots represent relative fold change compared with experimental control; quantification is normalized to actin (loading control).

3. Pharmacological applications

3.1 MB protection of hepatocyte and liver, and the role of PKA

Above sections have demonstrated that PKA mediated the dual GSK3β inhibition by MB. Following study then focused on the pharmacological applications of MB for preventing hepatocyte injury. To determine whether MB can protect cell against hepatocyte death, a previous published cell death model combining arachidonic acid (AA, 10 μM) and iron (5 μM) was used (Shin and Kim, 2009). MTT assay demonstrated that MB pretreatment could protect cells from the injury (Fig. 13A). Changes in the levels of apoptosis markers also cooperated with the cytoprotective effects of MB (Fig. 13B). In addition, GSH depletion, an indicator of ROS formation during apoptosis, was reversed by MB pretreatment (Fig. 13C), indicating MB can help maintaining redox homeostasis. Moreover, DCFH-DA assay indicated that MB could abolish AA + iron-increased H_2O_2 production (Fig. 13D). Taken together, these results support cytoprotective effects of MB. Additionally, whether PKA activity was altered in the MB's protective effect against AA + iron was demonstrated. Phosphorylation of PKA catalytic subunit at threonine residue is a key step for PKA activation (Steinberg et al., 1993), and current study demonstrated AA + iron stimuli lead a reduced PKA threonine phosphorylation, that can be reversed by MB pretreatment (Fig. 13E), being in line with the beneficial effect of PKA against ROS.

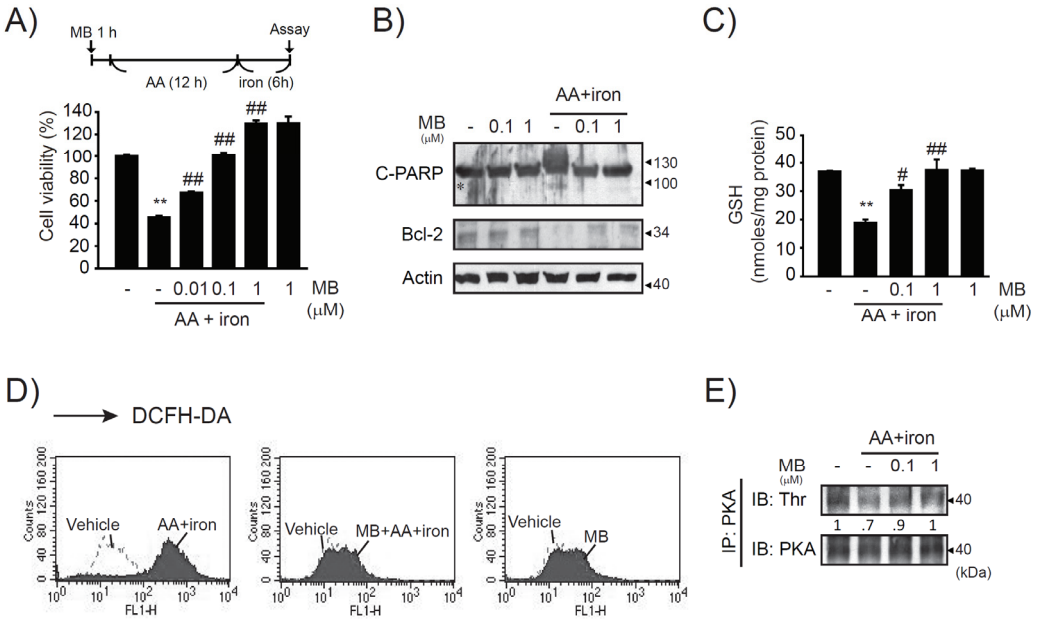

Figure 13. MB protects hepatocyte viability in a PKA-dependent manner

(A) HepG2 cells treated with 0.01-1 μM MB were incubated with 10 μM AA and were exposed to 5 μM iron as indicated. MTT assays were measured for cell viability.

(B) Immunoblottings of survival/apoptosis related markers in HepG2 cells treated as in panel A.

(C) Intracellular GSH content were measured.

(D) H_2O_2 production was determined by flow cytometry.

(E) PKA immunoprecipitates were measured with antibodies against phosphorylated threonine or PKA.

For A and C, data represent the mean ± SEM of three separate experiments. Significantly different as compared with experimental control: **P<0.01 or AA + iron group: #P<0.05, ##P<0.01.

Having demonstrated the *in vitro* cytoprotective effects of MB, then we wondered whether MB has similar protective effects in mice liver. To examine MB's ability on liver protection *in vivo*, the effects of MB on acute CCl_4 (48 h)-induced liver injury were determined in C57BL/6 mice. MB pretreatment significantly attenuated CCl_4-induced liver injury as shown from the improved H&E staining (Fig. 14A), decreased serum ALT and AST activities (Fig. 14B). In addition, MB also antagonized the CCl_4-induced upregulation of serum TNFα and Interleukin 1 β (IL1β) (Fig. 14C), as well as liver inducible nitric oxide synthase (iNOS) and cyclooxygenase 2 (COX2) protein levels (Fig. 14D), suggesting the anti-inflammatory effects of MB. Overall, these results demonstrate that MB protects hepatocyte and liver bot *in vitro* and *in vivo* from toxicants induced injury.

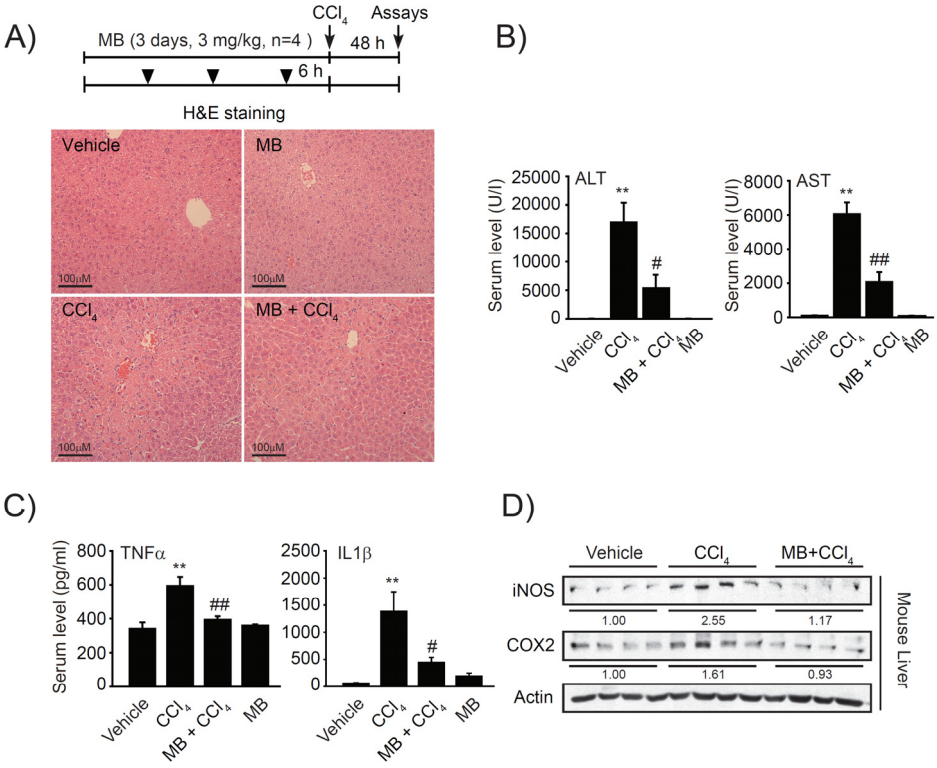

Figure 14. MB protects liver against CCl_4 induced injury

(A) Mice (n = 4/group) were orally administered with MB and were intraperitoneally injected with CCl_4 for 48 h. H&E staining were done on liver tissues.

(B) Serum ALT and AST activities.

(C) TNFα and IL1β contents in serum.

(D) Immunoblottings for iNOS and COX2 were done on liver homogenates.

For B and C, data represent the mean ± SEM. Significantly different as compared with experimental control: **P<0.01 or CCl_4 group: #P<0.05, ##P<0.01.

3.2 Liver protection by hepatocyte delivery of LXRα

Above sections have demonstrated LXRα's hepatocyte protective effects against TGFβ induced apoptosis, then, the impact of hepatocyte LXRα on cell survival and liver protection were examined. An albumin promoter-driven lentiviral vectors expressing control or LXRα (LV-Con^{alb} or LV-LXRα^{alb}) were employed to LXRα$^{-/-}$ mice liver, followed by multiple CCl_4 injection (4 weeks). Induction of LXRα was verified by qRT-PCR (Fig. 15A). In LV-LXRα^{alb} mice liver, attenuated hepatocyte and liver injury were observed, as shown from the results of TUNEL staining, H&E staining and immunoblottings of apoptosis/survival related markers (Fig. 15A). Concomitantly, elevated hepatic CB2, miR-27b and decreased USP4 by LV-LXRα^{alb} delivery were also observed (Fig. 15B). Finally, the hepatic mRNAs of inflammatory cytokines were significantly lessened (Fig. 15C). In conclusion, these data support the viewpoint that hepatocyte delivery of LXRα decreases hepatocyte and liver injury, emphasizing the important role of liver LXRα in hepatocyte protection.

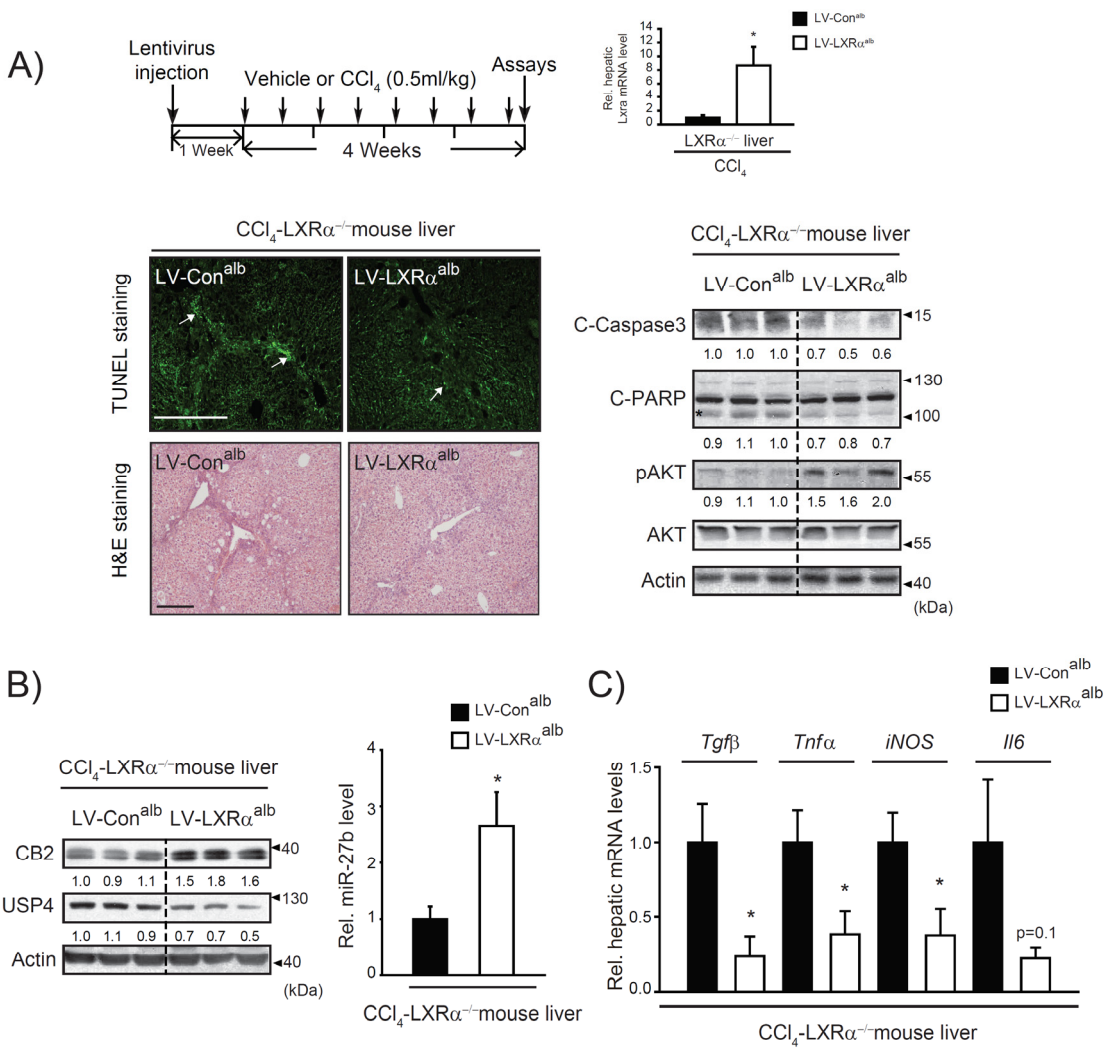

Figure 15. Hepatocyte delivery of LXRα attenuates CCl_4 induced liver injury

(A) One week after lentiviruses injection with control (LV-Con^{alb}) or LXRα (LV-LXRα^{alb}), liver injury were induced with multiple CCl_4 (0.5 mL/kg, 1:20 in corn oil) injection (n = 5/group, twice a week for 4 weeks). Hepatocyte apoptosis were determined by TUNEL staining and liver histology was observed by H&E staining (Scale bar = 100 μm) (left panel). Survival or apoptosis related proteins levels were

measured on mice livers (right panel). The level of LXRα was determined by qRT-PCR assays (insert panel).

(B) Left panel: protein levels of CB2 and USP4 were measured on the same mice liver samples as described in panel A. Right panel: the level of miR-27b was determined by qRT-PCR assays.

(C) qRT-PCR assays for proinflammation relation genes (*Tgfβ*, *Tnfα*, *iNOS* and *Il6*) were done on the same mouse liver samples as described in panel A.

For A-B, values below blots represent relative fold change compared with experimental control; quantification is normalized to actin (loading control). For A-C, data represent the mean ± SEM. Significantly different as compared with experimental control: *P<0.05.

IV. Discussion

Acute and chronic liver injury is a growing worldwide problem. Hepatocyte death is a major reason to cause liver diseases (Feldstein et al., 2003; Natori et al., 2001; Malhi et al., 2010). Hepatocyte, the predominant liver cell, is especially vulnerable to different toxic injuries due to its central role in xenobiotic metabolism including drugs, nutrient metabolism and the enterohepatic circulation of bile acids (Malhi et al., 2010). Different injuries on the liver activate the oxidative stress response and trigger hepatocyte death signaling pathways, which can cause activation of other types of cells (e.g., macrophage and hepatic stellate cell) to progress liver to inflammation, fibrosis and irreversible damage (Martin-Murphy et al., 2010; Watanabe et al., 2007). Thus, a tight regulation of functional hepatocyte may determine cell fate and organism survival.

PKA is a cAMP-dependent kinase and a fast signal sensor that plays a key role in signal transduction and energy metabolism regulation. PKA has been demonstrated to be protective in suppressing ROS formation via phosphorylating downstream substrates (e.g., pro-apoptotic protein BAD and mitochondrial fission mediator Drp1) (Harada et al., 1999; Cribbs and Strack, 2007). Also, antioxidant such as deferoxamine regulates cell survival through PKA activation (Ryu et al., 2005). Current study demonstrates that PKA mediates MB's molecular signaling transduction by regulating LKB1 activation and GSK3β inhibition. The results are consistent with the reports that PKA protects hepatocyte against death receptor-induced apoptosis and ischemia/reperfusion-mediated

liver injury (Wang et al., 2006; Ji et al., 2012).

MB has a more than 140 years' long history with various applications. MB can improve the hypotension associated with various clinical states (e.g., cardiac function in septic shock) (Preiser et al., 1995). It also decreases ethanol-induced fatty liver and improves liver cirrhosis and hepatopulmonary syndrome (Ryle et al., 1985; Schenk et al., 2000). Undoubtedly, evidence for its use in liver protection is limited but worth for more research. The current study used two approaches to measure MB's cytoprotective efficacy, 1) a severe oxidative stress cell model combining AA + iron, and 2) a toxicant induced acute hepatitis model in mice. Results revealed MB's bona fide effects in protecting hepatocytes both *in vitro* and *in vivo*, and provide a novel pharmacological effect of MB. GSK3β plays an important function in regulating cell cycle and apoptosis. GSK3β can be activated by oxidative stress, DNA damage or ER stress, and promotes cell apoptosis (Ngok-Ngam et al., 2013; Meares et al., 2011). By contrast, inhibition of GSK3β can improve mitochondrial function through regulating mitochondrial permeability transition pore (Petit-Paitel et al., 2009), and enables cell survival against ischemia/reperfusion injury (Park et al., 2006). Hence, GSK3β inhibition represents potential therapy for cell death. The present study demonstrate MB's ability in inhibiting GSK3β via dual phase-S9 phosphorylation controlled by PKA, consists with the beneficial role of PKA in maintaining cell viability.

Accumulating reports have suggested the beneficial effects and potential therapeutic values of LXRs on various disease including metabolic disorders, circulatory system diseases and cancer. LXR agonists improved insulin sensitivity in diabetic mice through inhibition of hepatic gluconeogenesis and increasing peripheral glucose uptake (Cao et al., 2003; Dalen et al., 2003). In another report, LXRs attenuated endotoxin-induced NAFLD liver injury in mouse via reducing TNFα and iNOS expression (Liu et al., 2012). In the field of circulatory system diseases, it is has been clearly established that LXRs activation result in relieving atherosclerosis. Attenuation of atherosclerosis by LXR agonists are associated with decreased inflammatory genes, reduced total cholesterol, increased HDL cholesterol, inhibition of vascular smooth muscle cell proliferation, as well as modulation on the plaque (Levin et al., 2005; Peng et al., 2008; Blaschke et al., 2004; Kratzer et al., 2009). LXRα has a cardioprotective effect against ischemia/reperfusion injury through reducing endoplasmic reticulum stress and ROS generation (He et al., 2014). Besides, LXRs have also been reported can attenuated diabetic cardiomyopathy and myocardial hypertrophy (Huynh et al., 2014; Kuipers et al., 2010). Increasing research have suggested that LXRs may be a potential therapeutic anti-tumor target against many cancer types such as breast, colon and prostate cancer (Chuu and Lin, 2010; El Roz et al., 2012; Lo Sasso et al., 2013). Similarly, LXRα suppressed HCC cell proliferation through downregulating forkhead box protein M1 protein, a transcription factor mastering cell cycle progression (Hu et al., 2014).

According to a recent report, LXR expression is lower in HCC patients, and prognosis analysis demonstrated that the lower LXR expression is associated with decreased overall survival rate in HCC patients (Long et al., 2017), suggesting LXR level can be used as a clinical marker for hepatocellular carcinoma prediction. All these above mentioned beneficial effects of LXRs demonstrate a broad spectrum of LXRs' clinical applications for various disease. However, the lipogenesis induced by LXR agonists actually impeded the application LXRα as therapeutic strategy for disease treatment, therefore it is required to explore more detailed molecular mechanism downstream of LXRα (e.g., certain genes that can be regulated by LXRα) that will be helpful to develop specific LXRα modulators with minimal side effects.

Current study demonstrated a novel function of LXRα on the regulation of hepatocyte survival. By using human and mouse GEO database available in public domain, we found the expression of LXRα was significantly downregulated in several liver injury models. Hence, dysregulation of LXRα may contribute to progression of liver injury. Moreover, LXRα agonist treatment reduces the extent of liver hepatocyte injury, whereas LXRα$^{-/-}$ mice are more susceptible to the toxic insult induced hepatocyte death. Our findings elucidate a protective role of LXRα in preventing hepatocyte death caused by toxicant, which is consistent with the report that LXRα prevents toxicant induced liver injury via cholesterol homeostasis regulation (Saini et al., 2011). Since LXRα is known in regulating hepatic fatty acid biosynthesis, current findings provide

the notion that a basal expression and activation of LXRα is required for hepatocyte survival, whereas overactivated LXRα signaling will ultimately leads to liver steatosis. Thus, a balanced regulation of LXRα is important for hepatocyte viability and prevention of liver injury.

Exposure of liver to toxicant such as CCl_4 may lead to hepatocyte injury through various proinflammatory cytokines. The cytokine networks have been implicated in mediating the hepatic response to injury stimuli (Russmannet al., 2010). In our study, by analyzing hepatic gene expression profiles in LXR knockout mice from GEO database (GSE38083), we observed that TGFβ signaling (TGFBR1 and TGFBR2) appeared as a link in the core network extracted from the upregulated DEGs by LXR knockdown. The analysis allowed us to assume that LXRα may exert its cytoprotective role via inhibition of TGFβ signaling, which was supported by our results that LXRα activation rescues hepatocytes from TGFβ induced death in both AML12 cells and mouse primary hepatocytes. LXRα inhibition of TGFβ signaling parallels the observation that TGFβ induced more apoptosis in mouse primary hepatocytes from LXRα$^{-/-}$ mice. Liver TGFβ level was significantly upregulated by CCl_4 (Jeon et al., 1997), in line with the report that TGFβ signaling participated in ROS production and promote hepatocyte damage (Black et al., 2007). Therefore, inhibition of TGFβ signaling will provide therapeutic rationale for drug intoxication along with hepatocyte damage. Here, our identification of TGFβ inhibition by LXRα provides a therapeutic rational of using LXRα as a strategy

for preventing hepatocyte apoptosis.

CB2 activation has liver protective effects including limiting liver fibrosis (Muñoz-Luque et al., 2008) and preventing alcohol-induced steatosis and inflammation (Louvet et al., 2011). Little is known about the mechanism regulating CB2 level. Understanding this molecular basis is important from a therapeutic standpoint. Here, we identify that LXRα upregulates CB2 in hepatocytes and contributes to hepatocyte protection. Importantly, CB2 inverse agonist SR144528 reversed the effects of GW3965 against TGFβ induced cell death, suggesting the requirement of CB2 in LXRα's hepatocyte protection. Our data strengthen the concept that LXRα activation, via CB2 induction, plays a critical role in antagonizing hepatocyte apoptosis.

It has been shown that inhibition of TβRI in hepatocytes diminished CCl_4 induced liver damage (Karkampouna et al., 2016), suggestive of TβRI facilitates hepatocyte injury. Here, we show that LXRα activation increases TβRI ubiquitination and destabilization in a CB2-dependent manner. USP4 have been identified as deubiquitylating enzyme of TβRI and strongly induce TGFβ signaling by maintaining sustained TβRI levels (Zhang et al., 2012). Our results of USP4 repression by LXRα or CB2 agonist supports the idea that LXRα-CB2 negative regulate USP4, which probably results to the decreased TβRI protein stability. In this study, we discovered USP4 as a novel target for miR-27b. MiR-27b has been widely studied in cancer research and is considered as both tumor suppressor and oncogene (Sun et al., 2016; Matsuyama et al.,

2016;) depending on different cancer type, indicating a complicated character of this microRNA. Consistent with our finding that miR-27b negatively regulate USP4 and TβRI, a recent publication identified that miR-27b has anti-fibrotic property in pulmonary fibroblasts by directly targeting to TβRI and Smad2 (Zeng et al., 2017). By contrast, in mouse pancreatic microvascular endothelial cells, miR-27b was increased by TGFβ and positively regulates TGFβ-mediated endothelial-mesenchymal transition (Suzuki et al., 2017). All these studies support a complex, direct or indirect regulatory mechanism of TGFβ signaling by miR-27b.

The cAMP/PKA signaling is involved in the modulation of intracellular pathways related with homeostasis in hepatocytes. For example, PKA inhibits lipogenesis by phosphorylating and repressing SREBP-1c and ChREBP (Lu and Shyy, 2006; Kawaguchi et al., 2001). PKA has been involved in mediating hepatic secretion of FGF21, a novel metabolic regulator in improving glucose tolerance and insulin sensitivity (Cyphert et al., 2014). Thus, PKA signaling is important for the integration of metabolic homeostasis in hepatocytes. In this study, the activity of PKA was mildly but significantly increased by treatment of LXRα agonist, being in line with the report of enlarged PKA-mediated downstream molecular signaling events by LXR agonist (Hsu et al., 2009). Moreover, our results that PKA was necessary for the suppression of USP4 and TβRI downstream of CB2, exhibited the role of PKA in mediating signal transduction downstream of LXRα-CB2. Another concern is that as a protein kinase, by

what kind of mechanism, PKA can regulate miR-27b. Studies have revealed that glucocorticoid receptor (GR) is an upstream transcriptional regulator for miR-27b expression (Kong et al., 2015). Interestingly, PKA can modulate the gene transcriptional ability of GR via enhancing the DNA binding activity of GR (Rangarajan et al., 1992). Thus, whether GR is involved in the regulation of miR-27b downstream of LXRα-CB2 mediated PKA activation require more experimental proofs.

Collectively, these findings demonstrate MB inhibits oxidative stress and toxicant-induced hepatocyte death and liver injury as the results of GSK3β inhibition, through direct PKA-dependent and indirect LKB1-AMPK mediated mechanism. In addition, LXRα limits hepatocyte apoptosis and contributes to the protection against liver damage via CB2 regulation. LXRα-CB2 prevents TGFβ induced hepatocyte injury, which is mediated by PKA-dependent USP4 inhibition. The present identifications uncover MB's bona fide effects and molecular basis for pharmacological application and additionally provide LXRα's regulatory pathway for hepatocyte viability. These results may provide new therapeutic targets for the prevention of hepatocyte death-associated liver disease.

V. Reference

Aggarwal K, Massagué J. Ubiquitin removal in the TGF-β pathway. *Nat Cell Biol* 2012;14:656-7.

Alston TA. Why does methylene blue reduce methemoglobin in benzocaine poisoning but beneficially oxidize hemoglobin in cyanide poisoning? *J Clin Anesth* 2014;26:702-3.

Apfel R, Benbrook D, Lernhardt E, *et al*. A novel orphan receptor specific for a subset of thyroid hormone-responsive elements and its interaction with the retinoid/thyroid hormone receptor subfamily. *Mol Cell Biol* 1994;14:7025-35.

Atamna H, Nguyen A, Schultz C, *et al*. Methylene blue delays cellular senescence and enhances key mitochondrial biochemical pathways. *FASEB J* 2008;22:703-12.

Bedikian AY, Garbe C, Conry R, *et al*. Dacarbazine with or without oblimersen (a Bcl-2 antisense oligonucleotide) in chemotherapy-naive patients with advanced melanoma and low-normal serum lactate dehydrogenase: 'The AGENDA trial'. *Melanoma Res* 2014;24:237-43.

Beaven SW, Wroblewski K, Wang J, *et al*. Liver X receptor signaling is a determinant of stellate cell activation and susceptibility to fibrotic liver disease. *Gastroenterology* 2011;140:1052-62.

Black D, Lyman S, Qian T, *et al*. Transforming growth factor beta mediates hepatocyte apoptosis through Smad3 generation of reactive oxygen species. *Biochimie*

2007;89:1464-73.

Blaschke F, Leppanen O, Takata Y, *et al*. Liver X receptor agonists suppress vascular smooth muscle cell proliferation and inhibit neointima formation in balloon-injured rat carotid arteries. *Circ Res* 2004;95:e110-23.

Börner C, Smida M, Höllt V, *et al*. Cannabinoid receptor type 1- and 2-mediated increase in cyclic AMP inhibits T cell receptor-triggered signaling. *J Biol Chem* 2009;284:35450-60.

Cao G, Liang Y, Broderick CL, *et al*. Antidiabetic action of a liver x receptor agonist mediated by inhibition of hepatic gluconeogenesis. *J Biol Chem* 2003;278:1131-6.

Chaube B, Malvi P, Singh SV, *et al*. AMPK maintains energy homeostasis and survival in cancer cells via regulating p38/PGC-1α-mediated mitochondrial biogenesis. *Cell Death Discov* 2015;1:15063.

Choi SH, Kim YW, Kim SG. AMPK-mediated GSK3beta inhibition by isoliquiritigenin contributes to protecting mitochondria against iron-catalyzed oxidative stress. *Biochem Pharmacol* 2010;79:1352-62.

Chu K, Miyazaki M, Man WC, *et al*. Stearoyl-coenzyme A desaturase 1 deficiency protects against hypertriglyceridemia and increases plasma high-density lipoprotein cholesterol induced by liver X receptor activation. *Mol Cell Biol* 2006;26:6786-98.

Chuu CP, Lin HP. Antiproliferative effect of LXR agonists T0901317 and 22(R)-hydroxycholesterol on multiple human cancer cell lines. *Anticancer Res*

2010;30:3643-8.

Collins SP, Reoma JL, Gamm DM, *et al*, LKB1, a novel serine/threonine protein kinase and potential tumour suppressor, is phosphorylated by cAMP-dependent protein kinase (PKA) and prenylated in vivo. *Biochem J* 2000;345:673-80.

Cribbs JT, Strack S. Reversible phosphorylation of Drp1 by cyclic AMP-dependent protein kinase and calcineurin regulates mitochondrial fission and cell death. *EMBO Rep* 2007;8:939-44.

Cyphert HA, Alonge KM, Ippagunta SM, *et al*. Glucagon stimulates hepatic FGF21 secretion through a PKA- and EPAC-dependent posttranscriptional mechanism. *PLoS One* 2014;9:e94996.

Dalen KT, Ulven SM, Bamberg K, *et al*. Expression of the insulin-responsive glucose transporter GLUT4 in adipocytes is dependent on liver X receptor alpha. *J Biol Chem* 2003;278:48283-91.

Ducheix S, Podechard N, Lasserre F, *et al*. A systems biology approach to the hepatic role of the oxysterol receptor LXR in the regulation of lipogenesis highlights a cross-talk with PPARα. *Biochimie* 2013;95:556-67.

El Roz A, Bard JM, Huvelin JM, *et al*. LXR agonists and ABCG1-dependent cholesterol efflux in MCF-7 breast cancer cells: relation to proliferation and apoptosis. *Anticancer Res* 2012;32:3007-13.

Fang X, Yu SX, Lu Y, *et al*. Phosphorylation and inactivation of glycogen synthase

kinase 3 by protein kinase A. *Proc Natl Acad Sci U S A* 2000; 97: 11960-5.

Feldstein AE, Canbay A, Angulo P, *et al*. Hepatocyte apoptosis and fas expression are prominent features of human nonalcoholic steatohepatitis. *Gastroenterology* 2003;125:437-43.

Fischer U, Schulze-Osthoff K. Apoptosis-based therapies and drug targets. *Cell Death Differ* 2005;1:942-61.

Francis SH, Corbin JD. Structure and function of cyclic nucleotide-dependent protein kinases. *Annu Rev Physiol* 1994;56:237-72.

Gabrielli D, Belisle E, Severino D, *et al*. Binding, aggregation and photochemical properties of methylene blue in mitochondrial suspensions. *Photochem Photobiol* 2004;79:227-32.

Hall C, Troutman SM, Price DK, *et al*. Bcl-2 family of proteins as therapeutic targets in genitourinary neoplasms. *Clin Genitourin Cancer* 2013;11:10-9.

Hardie DG, Ross FA, Hawley SA. AMPK: a nutrient and energy sensor that maintains energy homeostasis. *Nat Rev Mol Cell Biol* 2012;13:251-62.

Han CY, Lim SW, Koo JH, *et al*. PHLDA3 overexpression in hepatocytes by endoplasmic reticulum stress via IRE1-Xbp1s pathway expedites liver injury. *Gut* 2016;65:1377-88.

Harada H, Becknell B, Wilm M, *et al*. Phosphorylation and inactivation of BAD by mitochondria-anchored protein kinase A. *Mol Cell* 1999;3:413-22.

Hawley SA, Boudeau J, Reid JL, *et al*. Complexes between the LKB1 tumor suppressor, STRAD alpha/beta and MO25 alpha/beta are upstream kinases in the AMP-activated protein kinase cascade. *J Biol* 2003;2:28.

He Q, Pu J, Yuan A, *et al*. Activation of liver-X-receptor α but not liver-X-receptor β protects against myocardial ischemia/reperfusion injury. *Circ Heart Fail* 2014;7:1032-41.

Heo MJ, Kim YM, Koo JH, *et al*. microRNA-148a dysregulation discriminates poor prognosis of hepatocellular carcinoma in association with USP4 overexpression. *Oncotarget* 2014;5:2792-806.

Hirsch T, Marchetti P, Susin SA, *et al*. The apoptosis-necrosis paradox. Apoptogenic proteases activated after mitochondrial permeability transition determine the mode of cell death. *Oncogene* 1997;15:1573-81.

Hsu JJ, Lu J, Huang MS, *et al*. T0901317, an LXR agonist, augments PKA-induced vascular cell calcification. *FEBS Lett* 2009;583:1344-8.

Hu C, Liu D, Zhang Y, *et al*. LXRα-mediated downregulation of FOXM1 suppresses the proliferation of hepatocellular carcinoma cells. *Oncogene* 2014;33:2888-97.

Huang da W, Sherman BT, Lempicki RA. Systematic and integrative analysis of large gene lists using DAVID bioinformatics resources. *Nat Protoc* 2009;4:44-57.

Hurley RL, Anderson KA, Franzone JM, *et al*. The Ca2+/calmodulin-dependent protein kinase kinases are AMP-activated protein kinase kinases. *J Biol Chem*

2005;280:29060-6.

Huynh K, Bernardo BC, McMullen JR, *et al*. Diabetic cardiomyopathy: mechanisms and new treatment strategies targeting antioxidant signaling pathways. *Pharmacol Ther* 2014;142:375-415.

Iimuro Y, Gallucci RM, Luster MI, *et al*. Antibodies to tumor necrosis factor alfa attenuate hepatic necrosis and inflammation caused by chronic exposure to ethanol in the rat. *Hepatology* 1997;26:1530-7.

Inokuchi S, Aoyama T, Miura K, *et al*. Disruption of TAK1 in hepatocytes causes hepatic injury, inflammation, fibrosis, and carcinogenesis. *Proc Natl Acad Sci U S A* 2010;107:844-9.

Jeon SM, Chandel NS, Hay N. AMPK regulates NADPH homeostasis to promote tumour cell survival during energy stress. *Nature* 2012;485:661-5.

Jeon YJ, Han SH, Yang KH, *et al*. Induction of liver-associated transforming growth factor beta 1 (TGF-beta 1) mRNA expression by carbon tetrachloride leads to the inhibition of T helper 2 cell-associated lymphokines. *Toxicol Appl Pharmacol* 1997;144:27-35.

Ji H, Shen XD, Zhang Y, *et al*. Activation of cyclic adenosine monophosphate-dependent protein kinase a signaling prevents liver ischemia/reperfusion injury in mice. *Liver Transpl* 2012;18:659-70.

Joseph SB, Castrillo A, Laffitte BA, *et al*. Reciprocal regulation of inflammation and

lipid metabolism by liver X receptors. *Nat Med* 2003;9:213-9.

Joseph SB, Laffitte BA, Patel PH, *et al*. Direct and indirect mechanisms for regulation of fatty acid synthase gene expression by liver X receptors. *J Biol Chem* 2002;277:11019-25.

Kang SG, Lee WH, Lee YH, *et al*. Hypoxia-inducible factor-1α inhibition by a pyrrolopyrazine metabolite of oltipraz as a consequence of microRNAs 199a-5p and 20a induction. *Carcinogenesis* 2012;33:661-9.

Karkampouna S, Goumans MJ, Ten Dijke P, *et al*. Inhibition of TGFβ type I receptor activity facilitates liver regeneration upon acute CCl4 intoxication in mice. *Arch Toxicol* 2016;90:347-57.

Kawaguchi T, Takenoshita M, Kabashima T, *et al*. Glucose and cAMP regulate the L-type pyruvate kinase gene by phosphorylation/dephosphorylation of the carbohydrate response element binding protein. *Proc Natl Acad Sci U S A* 2001;98:13710-5.

Kennedy MA, Barrera GC, Nakamura K, *et al*. ABCG1 has a critical role in mediating cholesterol efflux to HDL and preventing cellular lipid accumulation. *Cell Metab* 2005;1:121-31.

Kim AY, Lee CG, Lee DY, *et al*. Enhanced antioxidant effect of prenylated polyphenols as Fyn inhibitor. *Free Radic Biol Med* 2012;53:1198-208.

Knabel MK, Ramachandran K, Karhadkar S, *et al*. Systemic delivery of scAAV8-

encoded miR-29a ameliorates hepatic fibrosis in carbon tetrachloride-treated mice. *PLoS One* 2015;10:e0124411.

Kohro T, Nakajima T, Wada Y, *et al*. Genomic structure and mapping of human orphan receptor LXR alpha: upregulation of LXRa mRNA during monocyte to macrophage differentiation. *J Atheroscler Thromb* 2000;7:145-51.

Kong X, Yu J, Bi J, *et al*. Glucocorticoids transcriptionally regulate miR-27b expression promoting body fat accumulation via suppressing the browning of white adipose tissue. *Diabetes* 2015;64:393-404.

Kratzer A, Buchebner M, Pfeifer T, *et al*. Synthetic LXR agonist attenuates plaque formation in apoE-/- mice without inducing liver steatosis and hypertriglyceridemia. *J Lipid Res* 2009;50:312-26.

Kuipers I, Li J, Vreeswijk-Baudoin I, *et al*. Activation of liver X receptors with T0901317 attenuates cardiac hypertrophy in vivo. *Eur J Heart Fail* 2010;12:1042-50.

Laffitte BA, Chao LC, Li J, *et al*. Activation of liver X receptor improves glucose tolerance through coordinate regulation of glucose metabolism in liver and adipose tissue. *Proc Natl Acad Sci U S A* 2003;100:5419-24.

Levin N, Bischoff ED, Daige CL, *et al*. Macrophage liver X receptor is required for antiatherogenic activity of LXR agonists. *Arterioscler Thromb Vasc Biol* 2005;25:135-42.

Li S, Hong M, Tan HY, *et al*. Insights into the role and interdependence of oxidative stress and inflammation in liver diseases. *Oxid Med Cell Longev* 2016;2016:4234061.

Liu Y, Han X, Bian Z, *et al*. Activation of liver X receptors attenuates endotoxin-induced liver injury in mice with nonalcoholic fatty liver disease. *Dig Dis Sci* 2012;57:390-8.

Lo Sasso G, Bovenga F, Murzilli S, *et al*. Liver X receptors inhibit proliferation of human colorectal cancer cells and growth of intestinal tumors in mice. *Gastroenterology* 2013;144:1497-507.

Long H, Guo X, Qiao S, *et al*. Tumor LXR expression is a prognostic marker for patients with hepatocellular carcinoma. *Pathol Oncol Res* 2017 May 16. [Epub ahead of print].

Louvet A, Teixeira-Clerc F, Chobert MN, *et al*. Cannabinoid CB2 receptors protect against alcoholic liver disease by regulating Kupffer cell polarization in mice. *Hepatology* 2011;54:1217-26.

Lu M, Shyy JY. Sterol regulatory element-binding protein 1 is negatively modulated by PKA phosphorylation. *Am J Physiol Cell Physiol* 2006;290:C1477-86.

Malhi H, Guicciardi ME, Gores GJ. Hepatocyte death: a clear and present danger. *Physiol Rev* 2010;90:1165-94.

Marquardt JU, Seo D, Gómez-Quiroz LE, *et al*. Loss of c-Met accelerates development

of liver fibrosis in response to CCl(4) exposure through deregulation of multiple molecular pathways. *Biochim Biophys Acta* 2012;1822:942-51.

Martin-Murphy BV, Holt MP, Ju C. The role of damage associated molecular pattern molecules in acetaminophen-induced liver injury in mice. *Toxicol Lett* 2010;192:387-94.

Matsuyama R, Okuzaki D, Okada M, *et al*. MicroRNA-27b suppresses tumor progression by regulating ARFGEF1 and focal adhesion signaling. *Cancer Sci* 2016;107:28-35.

Meares GP, Mines MA, Beurel E, *et al*. Glycogen synthase kinase-3 regulates endoplasmic reticulum (ER) stress-induced CHOP expression in neuronal cells. *Exp Cell Res* 2011;317:1621-8.

Muñoz-Luque J, Ros J, Fernández-Varo G, *et al*. Regression of fibrosis after chronic stimulation of cannabinoid CB2 receptor in cirrhotic rats. *J Pharmacol Exp Ther* 2008;324:475-83.

Natori S, Rust C, Stadheim LM, *et al*. Hepatocyte apoptosis is a pathologic feature of human alcoholic hepatitis. *J Hepatol* 2001;34:248-53.

Ngok-Ngam P, Watcharasit P, Thiantanawat A, *et al*. Pharmacological inhibition of GSK3 attenuates DNA damage-induced apoptosis via reduction of p53 mitochondrial translocation and Bax oligomerization in neuroblastoma SH-SY5Y cells. *Cell Mol Biol Lett* 2013;18:58-74.

Ohlow MJ, Moosmann B. Phenothiazine: the seven lives of pharmacology's first lead structure. *Drug Discov Today* 2011;16:119-31.

Oz M, Lorke DE, Petroianu GA. Methylene blue and Alzheimer's disease. *Biochem Pharmacol* 2009;78: 927-32.

Parascandola J. The theoretical basis of Paul Ehrlich's chemotherapy. *J Hist Med Allied Sci* 1981;36:19-43.

Park SS, Zhao H, Mueller RA, *et al*. Bradykinin prevents reperfusion injury by targeting mitochondrial permeability transition pore through glycogen synthase kinase 3beta. *J Mol Cell Cardiol* 2006;40:708-16.

Peet DJ, Turley SD, Ma W, *et al*. Cholesterol and bile acid metabolism are impaired in mice lacking the nuclear oxysterol receptor LXR alpha. *Cell* 1998;93:693-704.

Peng D, Hiipakka RA, Dai Q, *et al*. Antiatherosclerotic effects of a novel synthetic tissue-selective steroidal liver X receptor agonist in low-density lipoprotein receptor-deficient mice. *J Pharmacol Exp Ther* 2008;327:332-42.

Petit-Paitel A, Brau F, Cazareth J, *et al*. Involvment of cytosolic and mitochondrial GSK-3beta in mitochondrial dysfunction and neuronal cell death of MPTP/MPP-treated neurons. *PLoS One* 2009;4:e5491.

Pinkert CA, Ornitz DM, Brinster RL, *et al*. An albumin enhancer located 10 kb upstream functions along with its promoter to direct efficient, liver-specific expression in transgenic mice. *Genes Dev* 1987;1:268-76.

Preiser JC, Lejeune P, Roman A, *et al*. Methylene blue administration in septic shock: a clinical trial. *Crit Care Med* 1995;23:259-64.

Pockros PJ, Schiff ER, Shiffman ML, *et al*. Oral IDN-6556, an antiapoptotic caspase inhibitor, may lower aminotransferase activity in patients with chronic hepatitis C. *Hepatology* 2007;46:324-9.

Rangarajan PN, Umesono K, Evans RM. Modulation of glucocorticoid receptor function by protein kinase A. *Mol Endocrinol* 1992;6:1451-7.

Repa JJ, Liang G, Ou J, *et al*. Regulation of mouse sterol regulatory element-binding protein-1c gene (SREBP-1c) by oxysterol receptors, LXRalpha and LXRbeta. *Genes Dev* 2000a;14:2819-30.

Repa JJ, Turley SD, Lobaccaro JA, *et al*. Regulation of absorption and ABC1-mediated efflux of cholesterol by RXR heterodimers. *Science* 2000b;289:1524-9.

Russmann S, Jetter A, Kullak-Ublick GA. Pharmacogenetics of drug-induced liver injury. *Hepatology* 2010;52:748-61.

Ryle PR, Chakraborty J, Thomson AD. The effect of methylene blue on the hepatocellular redox state and liver lipid content during chronic ethanol feeding in the rat. *Biochem J* 1985;232:877-82.

Ryu H, Lee J, Impey S, *et al*. Antioxidants modulate mitochondrial PKA and increase CREB binding to D-loop DNA of the mitochondrial genome in neurons. *Proc Natl Acad Sci U S A* 2005;102:13915-20.

Saini SP, Zhang B, Niu Y, *et al*. Activation of liver X receptor increases acetaminophen clearance and prevents its toxicity in mice. *Hepatology* 2011;54:2208-17.

Sakurai K, Cederbaum AI. Oxidative stress and cytotoxicity induced by ferric-nitrilotriacetate in HepG2 cells that express cytochrome P450 2E1. *Mol Pharmacol* 1998;54:1024-35.

Schenk P, Madl C, Rezaie-Majd S, *et al*. Methylene blue improves the hepatopulmonary syndrome. *Ann Intern Med* 2000;133:701-6.

Schirmer RH, Adler H, Pickhardt M, *et al*. "Lest we forget you--methylene blue...". *Neurobiol Aging* 2011;32:2325.e7-16.

Schultz JR, Tu H, Luk A, *et al*. Role of LXRs in control of lipogenesis. *Genes Dev* 2000;14:2831-8.

Shaw RJ, Lamia KA, Vasquez D, *et al*. The kinase LKB1 mediates glucose homeostasis in liver and therapeutic effects of metformin. *Science* 2005;310:1642-6.

Shin SM, Kim SG. Inhibition of arachidonic acid and iron-induced mitochondrial dysfunction and apoptosis by oltipraz and novel 1,2-dithiole-3-thione congeners. *Mol Pharmacol* 2009;75:242-53.

Steinberg RA, Cauthron RD, Symcox MM, *et al*. Autoactivation of catalytic (C alpha) subunit of cyclic AMP-dependent protein kinase by phosphorylation of threonine 197. *Mol Cell Biol* 1993;13:2332-41.

Sun XF, Sun JP, Hou HT, *et al*. MicroRNA-27b exerts an oncogenic function by

targeting Fbxw7 in human hepatocellular carcinoma. *Tumour Biol* 2016;37:15325-32.

Suzuki HI, Katsura A, Mihira H, *et al*. Regulation of TGF-β-mediated endothelial-mesenchymal transition by microRNA-27. *J Biochem* 2017;161:417-20.

Takehara T, Tatsumi T, Suzuki T, *et al*. Hepatocyte-specific disruption of Bcl-xL leads to continuous hepatocyte apoptosis and liver fibrotic responses. *Gastroenterology* 2004;127:1189-97.

Tangirala RK, Bischoff ED, Joseph SB, *et al*. Identification of macrophage liver X receptors as inhibitors of atherosclerosis. *Proc Natl Acad Sci U S A* 2002;99:11896-901.

Tilg H, Jalan R, Kaser A, *et al*. Anti-tumor necrosis factor-alpha monoclonal antibody therapy in severe alcoholic hepatitis. *J Hepatol* 2003;38:419-25.

Uppal H, Saini SP, Moschetta A, *et al*. Activation of LXRs prevents bile acid toxicity and cholestasis in female mice. *Hepatology* 2007;45:422-32.

Venkateswaran A, Laffitte BA, Joseph SB, *et al*. Control of cellular cholesterol efflux by the nuclear oxysterol receptor LXR alpha. *Proc Natl Acad Sci U S A* 2000;97:12097-102

Visarius TM, Stucki JW, Lauterburg BH. Inhibition and stimulation of long-chain fatty acid oxidation by chloroacetaldehyde and methylene blue in rats. *J Pharmacol Exp Ther* 1999;289:820-4.

Xie Z, Zhang J, Wu J, *et al*. Upregulation of mitochondrial uncoupling protein-2 by the AMP-activated protein kinase in endothelial cells attenuates oxidative stress in diabetes. *Diabetes* 2008;57:3222-30.

Wall EA, Zavzavadjian JR, Chang MS, *et al*. Suppression of LPS-induced TNF-alpha production in macrophages by cAMP is mediated by PKA-AKAP95-p105. *Sci Signal* 2009;2:ra28.

Wang Y, Kim PK, Peng X, *et al*. Cyclic AMP and cyclic GMP suppress TNFalpha-induced hepatocyte apoptosis by inhibiting FADD up-regulation via a protein kinase A-dependent pathway. *Apoptosis* 2006;11:441-51.

Wang Y, Rogers PM, Stayrook KR, *et al*. The selective Alzheimer's disease indicator-1 gene (Seladin-1/DHCR24) is a liver X receptor target gene. *Mol Pharmacol* 2008;74:1716-21.

Watanabe A, Hashmi A, Gomes DA, *et al*. Apoptotic hepatocyte DNA inhibits hepatic stellate cell chemotaxis via toll-like receptor 9. *Hepatology* 2007;46:1509-18.

Weinstein J, Scott A, Hunter Fe Jr. The action of gramicidin d on isolated liver mitochondria. *J Biol Chem* 1964;239:3031-7.

Wu HM, Lee CG, Hwang SJ, *et al*. Mitigation of carbon tetrachloride-induced hepatic injury by methylene blue, a repurposed drug, is mediated by dual inhibition of GSK3β downstream of PKA. *Br J Pharmacol* 2014;171:2790-802.

Yang YM, Lee CG, Koo JH, *et al*. Gα12 overexpressed in hepatocellular carcinoma

reduces microRNA-122 expression via HNF4α inactivation, which causes c-Met induction. *Oncotarget* 2015;6:19055-69.

Zeng X, Huang C, Senavirathna L, *et al*. miR-27b inhibits fibroblast activation via targeting TGFβ signaling pathway. *BMC Cell Biol* 2017;18:9.

Zhang L, Zhou F, Drabsch Y, *et al*. USP4 is regulated by AKT phosphorylation and directly deubiquitylates TGF-β type I receptor. *Nat Cell Biol* 2012;14:717-26.

VI. 국문요약

간세포 생존의 PKA 연계 조절 경로와 약물학적 응용

우 홍 민

지도교수: 김 상 건

약물, 알코올 그리고 바이러스와 같은 독성 물질에 의해 간세포가 주로 영향을 받게 된다. 간세포의 죽음은 약물에 의한 간 손상부터 바이러스/알코올/자가면역성 간염, 그리고 대사 질환에 이르기까지 다양한 간질환에 있어 흔하게 나타나는 현상이다. 따라서 간세포의 기능을 유지하는 것은 간질환의 치료와 예방에 있어 중요하다. 하지만 아직까지 간세포의 죽음을 제어할 수 있는 타겟에 대한 접근은 임상적으로 쉽지 않다. 따라서 간세포의 생존과 관련된 신호 경로 또는 분자 타겟에 대한 연구가 더 필요하다. PKA는 cAMP 의존적 효소로 수용체/치료 약물과 세포내 타겟 사이의 분자 신호 전송을 매개한다. PKA와 관련된 수많은 타겟의 보고는 에너지 대사에 있어 PKA가 중요한 조절 인자임을 의미한다. 본 연구에서는 간세포의 생존을 타겟하는 PKA 신호 경로와 연관된 새로운 분자들을 탐색하고, 분자의 조절 신호를 탐구하고자 하였다.

PKA와 연관된 신호 경로를 조절할 수 있는 약물을 발굴하기 위해, 본 연구에서는 methylene blue (MB)의 간세포 보호 효과를 연구하였다. MB는 미토콘드리아를 목표하는 약물이다. MB 처치는 PKA를 통해 LKB1를 활성화시켰고, LKB1을 매개한 AMPK의 활성화는 GSK3β의 활성을 억제하였다. 게다가 MB 처리는 AMPK 비의존적으로 초기에 GSK3β의 억제를 유발했다. siRNA로 PKA를 억제하였을 때에는 MB에 의한 GSK3β를 억제를 관찰할 수 없었다. 이는 MB에 의한 초기 GSK3β의 억제 또한 PKA 의존적임을 의미한다. MB가 독성물질에 의한 간세포 손상을 억제할 수 있음을 *in vitro* 또는 *in vivo* 실험으로 증명하였다. 이러한 결과들은 MB가 PKA를 매개한 GSK3β 이중 억제 통로를 통해 간세포를 보호함을 지지한다.

LXRα는 핵 수용체에 속하며, 지질 대사와 염증 조절에 관여한다. 독성물질을 처치한 간세포 및 동물의 간조직, 그리고 간질환 환자의 GEO database를 분석한 결과, LXRα의 발현이 현저히 감소하였다. LXRα agonist 투여는 CCl_4에 의한 간세포 손상을 개선시킨 반면, LXRα$^{-/-}$ 동물은 CCl_4에 의한 간세포 죽음 및 간 손상이 더 심했다. 이는 LXRα가 간세포를 보호하는 효과를 가짐을 의미한다. 다른 bioinformatics 분석을 통해 LXRα가 TGFβ를 억제함으로써 간세포를 보호할 수 있으며, 이는 AML12 세포주와 마우스에서 분리한 간세포를 이용하여 증명하였다. Immunoblottings, qRT-PCR, reporter gene assays와 ChIP analyses를 시행하여 LXRα의 하위 분자 기전을 연구했다. 본 연구에서 cannabinoid receptor 2 (CB2)가 LXRα의 전사 타겟임을 발견했다. CB2

는 miR-27b를 증가시켜 간세포 보호 효과를 나타내었다. 또한 miR-27b가 TGFβ receptor I의 deubiquitylating 효소인 USP4의 상위 조절 인자임을 발견하였다. 렌티바이러스를 이용하여 LXRα를 간세포 선택적으로 과발현 시켰을 때 간세포 손상은 개선되었다. 이상의 결과들은 LXRα가 전사적으로 CB2를 증가시켜 miR-27b를 유도함으로써 USP4를 억제하여 간세포 보호 효과를 나타냄을 보여준다.

결론적으로, 본 연구는 약물을 통한 PKA 의존적 LKB1-AMPK 신호 회로 간세포 보호에 기여함을 제시하였다. 또한 LXRα 하위로 CB2를 매개한 PKA 신호 활성화를 통한 간세포의 보호 기전을 발견하였다. 이를 통해 간세포의 손상 및 간질환의 치료에 새로운 치료타겟 발굴 및 약물학적 응용이 가능할 것으로 기대한다.

주요어: 간세포손상, PKA, LXRα, CB2, Methylene blue, AMPK

학번: 2009-24034